Evaluated Theoretical Cross-Section Data for Charge Exchange of Multiply Charged Ions with Atoms. III. Nonhydrogenic Target Atoms

Cite as: Journal of Physical and Chemical Reference Data **13**, 1199 (1984); https://doi.org/10.1063/1.555727
Published Online: 15 October 2009

R. K. Janev, and J. W. Gallagher

Evaluated Theoretical Cross-Section Data for Charge Exchange of Multiply Charged Ions with Atoms. III. Nonhydrogenic Target Atoms

R. K. Janev[a] and J. W. Gallagher

Joint Institute for Laboratory Astrophysics, University of Colorado and National Bureau of Standards, Boulder, Colorado 80309

The theoretical cross-section data for single-electron capture in collisions of multiply charged ions with nonhydrogenic atoms are compiled and their accuracy is assessed. The energy per unit mass range considered is from ~ 1 eV/u to several MeV/u, u being the unified atomic mass unit. Accuracy is assessed using both pure theoretical arguments and comparison with experimental data, where available. A similar assessment is performed for the two-electron capture cross-section data in ion–atom collisions, as well as for single- and double-charge exchange in ion–ion collisions.

Key words: charge exchange; cross sections; electron capture; ion–atom collisions; ion–ion collisions; multiply charged ions.

Contents

List of Tables

List of Figures

[a] Permanent address: Institute of Physics, Belgrade, Yugoslavia.

1. Introduction

In the previous two papers of this series,[1,2] we have presented evaluated theoretical cross-section data for the charge exchange process in collisions of hydrogen atoms with fully[1] and partially[2] stripped ions. In this paper, we continue our analysis of the existing theoretical charge exchange cross-section data to the case when the target is a nonhydrogenic atom,

$$A + B^{q+} \rightarrow A^{+} + B^{(q-1)+}, \quad A \neq H, \quad q \geqslant 2, \tag{1}$$

and B^{q+} may be any ion in a charge state with $2 \leqslant q \leqslant Z$, where Z is the nuclear charge of B. The energies in this paper are given in the form of the laboratory energy of the projectile ion (E) in eV (or keV, or MeV) divided by its mass (M) expressed in unified mass units (u). The energy per unit mass region included in our analysis extends from a few eV/u to several MeV/u. The overwhelming majority of cross-section calculations have been performed in this energy region. However, to be complete, when presenting the cross-section data sources, we go beyond these limits. For the same reason, in our present analysis we include also the existing theoretical cross-section data for the two-electron capture in ion–atom collisions,

$$A + B^{q+} \rightarrow A^{2+} + B^{(q-2)+}, \quad q \geqslant 2, \tag{2}$$

as well as the data for single- and double-charge transfer in the ion–ion collisions.

$$A^{q_1+} + B^{q_2+} \rightarrow A^{(q_1+i)+} + B^{(q_2-i)+},$$
$$q_2 \geqslant q_1, \quad q_2 \geqslant 2, \quad i = 1,2. \tag{3}$$

Compared with the hydrogen atom target case, the evaluation of theoretical charge exchange cross sections for multielectron target atoms is a considerably more difficult task. The difficulties, which are inherent in the cross-section calculations themselves, arise from two sources: complexity of the electronic structure of colliding system, and complexity of the collision dynamics. Accurate representation of the electronic states of a multielectron collision system is an extremely difficult problem in itself. For different regions of the collision energy, different representations of these states are appropriate (adiabatic, diabatic, atomic-state representations), and in their practical realization drastic approximations are often involved (e.g., inclusion of only the valence-shell electrons in the low-energy regime, or the inner-shell electrons at very high energies, or use of independent-particle models, etc.). The accuracy with which the electronic states are described is directly transferred into the accuracy of the cross-section calculations. Exclusion of the correlation effects may also have a significant influence on the accuracy of calculated cross sections, both at low and at high energies.

The multielectron character of a target atom introduces even more difficulties in the description of the collision dynamics. In a many-electron collision system, many new reaction channels not present in the one-electron systems become available, not only because of a greater multitude of interacting states, but also due to a diversity of multistep and multielectron correlated transition processes (such as simultaneous capture and excitation or ionization). When the projectile ion charge is high, the coupling of all these reaction channels may be strong at both low and high collision energies. Theoretical methods for treating multistep and electron-correlated processes are not well developed,[3] and for the processes involving simultaneous transitions of more than two electrons, they are nonexistent. Therefore, a full description of the charge exchange process in collisions of complex atoms with multicharged ions is a formidable problem, even in a restricted region of the collision energy. Practical cross-section calculations are usually based on significant approximations of collision dynamics or on suitable models, which can be justified only for particular collision systems and energy regions.

From the above discussion of the structural and dynamical complexity of multielectron collision systems, it follows that a proper evaluation of the existing calculated charge exchange cross sections for the reactions (1)–(3) is extremely difficult to perform. In one-electron systems (treated in Ref. 1), the electronic states are exactly known and highly accurate calculations are available (at least for a number of systems) against which the accuracy of different methods can be checked; however, in the present case, none of these circumstances exists. In only a few instances involving helium atom targets, such a comparative method, supplemented by comparison with experimental data, can be accomplished. In all other cases, the assessment of the accuracy of theoretical cross-section data can be based only on the intrinsic strength and limitations of the method applied, the analysis of the approximations made in the electronic structure description and in the treatment of the collision dynamics (e.g., the possible influence of neglected reaction channels), and comparison with experimental data where they exist. The experimental data and the most accurate calculations for the He-fully stripped ion reaction system can be used to determine the relative accuracies of different methods, which then may be extended to other collision systems. Such an approach does not represent a "critical evaluation" of the data for most of the reactions considered. However, it does provide a clue to estimate the expected accuracies in a plausible way.

In the next section, we give a brief presentation of the theoretical methods so far employed in the cross-section calculations of reactions (1)–(3), emphasizing the new aspects mentioned above. A review of the cross-section data calculations is given in Sec. 3. The criteria for assessing the expected accuracy of the existing cross-section data is discussed in more detail in Sec. 4. Finally, in Sec. 5, we present cross-section data with their assessed accuracy, and give details of how the accuracy assessments were performed for particular reactions or classes of them.

2. Theoretical Methods

2.1. One-Electron Capture

The theoretical methods for calculation of one-electron capture cross section in atom-multicharged ion collisions were described in Refs. 1 and 2. Those in which the symmetry properties of the one-electron diatomic system are explicitly used [such as the multichannel Landau–Zener model

(M-LZ-RC) or the analytic classical model (Cl-M-An)] are not applicable to the many-electron target (or projectile) case, since in the latter the symmetry is reduced. Other major differences between one-electron and many-electron targets, from the point of view of the theoretical methods discussed in Ref. 1, are the following:

(i) The low-energy molecular-orbital expansion close-coupling methods (CC-MO), as well as the medium-energy atomic-orbital expansion close-coupling methods (CC-AO), require a larger basis set to incorporate the larger number of coupling interactions present in the many-electron collision systems. In CC-MO methods, the determination of the electronic basis set, as well as the potential and dynamic coupling interactions is a prerequisite, which by itself may be a formidably complex problem.

(ii) At higher collision energies, the single- and two-electron capture processes may take place from the inner-electronic shells of the target atom, and may be accompanied by other electron transition processes (such as Auger excitation, ionization, etc.). Because of the complexity introduced in the treatment by (i) and (ii), the most-studied charge exchange reactions have been those involving a relatively small number of electrons in the colliding system and, in particular, reactions with He as a target atom.

As in Ref. 1, it is convenient to discuss the theoretical methods separately in three different regions of collision velocity: $v \ll v_e$, $v \sim v_e$, and $v \gg v_e$, where v_e is the characteristic (classical) velocity of the bound electron participating in the capture process. For the outer-shell electrons $v \sim v_0 = 2.19 \times 10^8$ cm/s, while for the inner-shell electrons $v_e \sim Z/n$, where Z is the nuclear charge of the target atom and n (~ 1) is the principal quantum number of the shell. For the heavy atoms, Z is large and the region $v \lesssim v_e$ may actually involve very high collision energies.

a. Low-Velocity Region ($v \lesssim v_e$)

The theoretical methods most frequently used for charge exchange cross-section calculations in this region are the CC-MO method, with or without inclusion of electron translation factors (ETF) in the basis functions [in the latter case CC-MO is called perturbed stationary state method (PSS)], the asymptotic method (AM) with model solutions of the two-state strong coupling problem [such as the Landau–Zener (LZ) model] and different versions of the decay model [the electron tunneling model, referred to as DM below, and the absorbing sphere model (ASM)]. The main features of these methods have been discussed in Ref. 1. Here we add that due to the larger number of reaction channels available for charge exchange when the target is a many-electron atom, the appropriateness of decay models for describing the process is considerably increased. Therefore, the accuracy of the results provided by these models is expected to be higher than in the one-electron target case. Another point which should be emphasized with the application of decay models in the case of a multielectron target atom is that their straightforward use gives the total cross section σ_{tot} for capture of one, two, three, etc., electrons from the target. Special procedures must be employed in order to separate the cross sections $\sigma_1, \sigma_2, \sigma_3, \ldots$ (for one, two, three, etc., electron captures) from σ_{tot}.[3] Only when $\sigma_2, \sigma_3, \ldots$ are small, the calculated σ_{DM} or σ_{ASM} cross sections can be expected to be close to σ_1. This is true, for example, for alkalis, when the first and the second ionization potentials are significantly different. (The opposite is true for inert gas atoms.) All σ_{DM}, except for $He + Ar^{6+}$ case,[3,4] are the same as σ_{tot} (see Table 1).

Most of the CC-MO calculations of single-electron capture cross sections in reaction (1) have used the PSS method. PSS cross-section calculations with an accuracy better than 50% have been done for $He + He^{2+}$ (16 coupled states),[5] $He + Be^{3+}$ (four states),[6] $He + B^{3+}$ (four states),[7] and $He + C^{4+}$ (five states).[6] Coupled-channel calculations with only two molecular states have also been performed, both numerically and with the Landau–Zener and Rapp–Francis (RF) models.[9,10] The accuracy of the CC-MO results is directly related to the size of the MO basis, the accuracy in solving the electronic structure part of the problem, and at higher energies, the adequacy of the ETFs in representing the electron momentum transfer effects (see Refs. 1 and 2).

For high values of the ionic charge q, the classical considerations of the electron capture process (1) and most of the experimental data suggest the following scaling rule for the cross section σ_{cx} at low energies[11]

$$\sigma_{cx} = (4.5 \pm 1) \times 10^{-16} N q \left(\frac{I_H}{I_0}\right)^2 \text{ cm}^2,$$

$$E\,(\text{keV/u}) \lesssim 15\, q \left(\frac{I_0}{I_H}\right), \tag{4}$$

where N is the number of valence electrons in the atom A, and I_0, I_H ($= 13.6$ eV) are the ionization potentials of A and the hydrogen atom, respectively. While the approximate linear dependence of σ_{cx} on q is well established (see, e.g., Ref. 12), the dependence of σ_{cx} on I_0 is still controversial.

The theoretical predictions and experimental observations of $\sigma_{cx} \sim I_0^{-\alpha}$ are dispersed between $\alpha = 1$ and $\alpha = 2$.[12] In most instances, Eq. (4) represents the data (if $q \gtrsim 10$) within an accuracy of $\pm$ 50%. The decay models predict a weak (logarithmic) dependence of σ_{cx} on E,[3] whereas for smaller values of q, σ_{cx} decreases with decreasing E due to the pronounced selectivity of the electron capture process.

b. Intermediate-Velocity Region ($v \sim v_e$)

The following methods have been applied for charge exchange cross-section calculations in the relative velocity region $v \approx (1\text{–}5)\, v_e$: the atomic-orbital close-coupling method, with or without inclusion of pseudostates, the unitarized distorted wave approximation (UDWA), the classical trajectory Monte Carlo (CTMC) method, and the Vainshtein–Presnyakov–Sobel'man method with semiempirical normalization (VPS-Emp). Since in this energy region capture from the inner shells starts to be important, the application of the CC-AO method requires predetermination of adequate atomic orbitals. The single-electron atomic orbitals can be generated by the Hartree–Fock method or by using some other procedure to account for the electron screening effects (the semiempirical Slater rules, the Herman–Skillman screening method,[13] the variable screening model,[14] etc.). With increasing the energy, higher excited states and the

ionization channel become increasingly important and must be represented in the basis set by adequately chosen pseudostates.[1] For the lower energies, where molecular effects are expected to play a role, pseudostates describing these effects may also be introduced in the expansion basis. Plane-wave ETF are usually considered as adequate for the region $v > v_e$.

The most extensive CC-AO calculations have been done for $Ne + He^{2+}$, and Li^{3+} with inclusion of 48 Hartree–Fock AOs in the basis,[15] for the $Ti + He^{2+}$, $Cu + He^{2+}$, C^{6+}, and O^{8+} systems[16] with a basis of 28 AO + pseudostates, and for the $Ar + C^{4+}$, C^{6+} systems[17] (AO + psuedostates), for electron capture from the inner K and L shells. Also in this category are the CC-AO calculations for $Li + He^{2+}$ system,[18] with a 40-state basis, including united atom pseudostates. In some cases, however, when the energy resonance condition is fulfilled, a two-state CC-AO scheme provides reasonably accurate cross-section results for the K–K electron capture.[19]

The application of the UDWA and CTMC methods to many-electron targets requires the introduction of an effective charge, Z_{eff}, for the ionic core of the atom; the uncertainty in the determination of Z_{eff} is directly reflected in the accuracy of the computed cross sections. The VPS method, which is essentially a two-state model for the charge exchange process, implies independent treatment of each target electronic shell and each final product state. An empirical factor of 1/3 is usually introduced in this method (VPS-Emp) to simulate the second-order effects. A theoretical justification for this factor (within the second Born approximation) can, however, be found only for the $1s \rightarrow 1s$ transitions. Therefore, the accuracy of this method is rather uncertain.

Due to the complexity of charge exchange dynamics in the intermediate velocity region (strong coupling of a large number of atomic discrete and continuum states), it is difficult to extract any information concerning the scaling relationships for the cross section σ_{cx}. In this region $\sigma_{cx} \sim q^{\beta}$, where β may have values between 1 and 3 and depends both on the relative velocity and the initial state electron binding energy (I_0). The dependence of σ_{cx} on I_0 is also unknown.

c. High-Velocity Region ($v > v_e$)

Many theoretical methods have been applied to the calculation of the cross section of reaction (1) in the high-velocity region. These include extension of the VPS-Emp method; the Brinkman–Kramers (BK) approximation, both in its conventional form and applying *ad hoc* normalization procedures either to the cross section (BK-Emp)[20] or to the transition probability (N-BK)[21]; the eikonal extension of the BK approximation (BK-Eik); the first Born (B1) approximation; the orthogonalized Bates–Born approximation (B-B1); and the continuum distorted wave (CDW) method. For sufficiently high collision velocities ($v \gtrsim 10$), the CDW approximation, in which the second-order scattering effects are accounted for, can provide cross sections with an accuracy of $\pm$ 30%, provided the initial and final bound states of the electron are adequately described (i.e., the electron correlation effects are adequately included in the target and product-ion wave functions). Due to the sensitivity of CDW method to the quality of the initial-state wave function, it has been applied so far only to the $He + He^{2+}$ system.[21–23] The results of the other high-velocity methods for charge exchange are also sensitive to the accuracy of the target electron wave function.

2.2. Electron Capture in Ion–Ion Collisions

The theoretical methods for treating the electron capture process in ion–ion collisions are the same as those for ion–atom collisions. The only difference is that in the former one has to incorporate the effects of the Coulomb repulsion explicitly in the treatment. Within the semiclassical approximation, these effects are accounted for by using Coulomb trajectories for the motion of the heavy particles. The Coulomb repulsion effects influence the total capture cross section only in the energy region $E \lesssim E_0 = q_1 q_2$, where q_1 and q_2 are the charges of the colliding ions. The effect is an exponential decrease of the cross section for $E < E_0$. For nonresonant electron capture reactions, this region lies in the domain of energies where the cross section already has an exponential decrease (with decreasing energy) due to the adiabatic character of the process. The Coulomb repulsion effects only enhance this decrease in the cross section. In resonant reactions, however, these effects are the only reason for the decrease of the cross section at low energies ($E < E_0$).

The number of theoretically studied charge exchange reactions for ion–ion collisions (listed in Table 2) is relatively small compared to that for ion–atom collisions. The following methods have been applied in the cross-section calculations: the two-state close-coupling models of the Landau–Zener, or Rosen–Zener–Demkov (RZD) type, and the asymptotic method for the resonant electron capture (AM-Res), the CTMC method, the Coulomb-projected Born (CPB) approximation, and the CDW method, each in the region of its validity. With the exception of CDW, all the above-mentioned methods provide results with a factor of 2 accuracy (or even worse), except when the colliding system possesses only one electron. Also in Table 2 are some reactions of two-electron capture in ion–ion collisions for which cross-section calculations have been made. The discussion in Sec. 2.1 regarding the influence of electronic structure on the accuracy of cross-section calculations also holds for ion–ion collisions.

For the resonant and quasiresonant electron capture reactions, the main dependences of the cross section on the projectile charge q_2 are[24–26]

$$\sigma_{cx}^{(i)} \sim q_2^{-\gamma}, \quad (\gamma \approx 2), \quad E \gtrsim q_1 q_2, \tag{5a}$$

$$\sim q_2^{n} e^{-\delta q_2^3}, \quad E \ll q_1 q_2, \tag{5b}$$

where $n > 1$ and δ is a constant (~ 2). For the resonant double-electron capture $\gamma = 1.7$.[25]

Cross-section calculations with an accuracy of better than $\pm$ 50% have been done for the $Ba^+ + Ba^+$ low-energy charge exchange using the CC-MO method[28] and for the He^+, Li^{2+}, $Be^{3+} + He^{2+}$ high-energy collisions using the CDW method.[24]

2.3. Two-Electron Capture Reactions

The two-electron and one-electron capture processes differ in that the former takes place between two-electron initial and final electronic configurations in the system. Since during the transitions, the two electrons are strongly correlated, the corresponding initial and final state wave functions must be appropriately determined. This aspect constitutes the main difficulty in treating the double-charge transfer process, and the degree of sophistication with which this problem is resolved is directly reflected in the accuracy of final results. Correlation effects between the transferring electrons may be neglected (independent electron model) only at very high collision energies.

Theoretical cross-section data for two-electron capture in atom-multicharged ion collisions are rather scarce, and most of them have been performed for a helium atom target (see Table 3). Almost all of the methods discussed in Sec. 2.1 have been applied to the double charge transfer process. Accurate cross-section data for the $He + He^{2+}$ system have been provided in the low-energy region by the PSS method with a 16 MO basis set,[5] and in the intermediate energy region by the CC-AO method employing a basis of nine states.[29] We note, however, that the existing experimental data for this system are rather incoherent, particularly in the low-energy region. Capture of two K-shell electrons from Ne and Ar by highly charged ions has also been studied by the CC-AO and CDW methods (see Table 3). Another extensively studied system is $He + C^{4+}$, for which cross sections have been produced both by the PSS method[6] and the asymptotic method.[30] More details about the theoretical methods for treating two-electron capture processes can be found in Ref. 3.

3. Review of Data Sources

The theoretical cross-section calculations for the single and double charge exchange processes in ion–atom and ion–ion collisions are reviewed in Tables 1–3. Only cross sections calculated after 1970 are included in these tables. The data produced prior to this period are either superseded by more recent calculations or (for the few which are not) can be found in the standard textbooks on atomic collisions. For each ion–atom or ion–ion collision pair, the following information is displayed in Tables 1–3: the reference of the data source, the energy range in which the calculations were carried out, the applied method, some comment on the calculations, and the assessed accuracy of the data.The criteria of this assessment are discussed in the next section.

4. Assessment Criteria and Procedure

We have adopted the same criteria for evaluating the accuracy of the computed cross sections as in our previous papers, Refs. 1 and 2. These are

(1) degree of sophistication of the calculations [i.e., size of the basis, inclusion and character of ETFs (when applicable), etc.];

(2) degree of the intrinsic accuracy of the applied method (i.e., number of channels included, convergence, appropriateness of basic assumptions, etc.);

(3) degree of agreement with the most reliable experimental data.

For a multielectron target, in addition to the above criteria one should also add

(4) the accuracy of representing electronic states and inter-electron correlations (the latter particularly for the two-electron capture reactions), and in the case of ion–ion charge exchange reactions also:

(5) the account of the Coulomb trajectory effects in the calculations.

As in Refs. 1 and 2, we adopt the following rating scheme for the accuracies of the computational methods and cross-section results:

Category	Accuracy
(a)	Better than $\pm$ 20%
(b)	$\pm$ 20%–$\pm$ 50%
(c)	$\pm$ 50%–$\pm$ 100%
(d)	Worse than 100%

By applying criteria (1)–(3) to the methods used for cross-section calculations in one-electron systems, one arrives at the accuracy which each of the methods can provide in the velocity region of its validity; these are presented in Table 4 (taken from Ref. 1 and somewhat extended). The assessment procedure includes a comparative analysis of the results of different methods for systems for which both experimental and theoretical results exist with an accuracy of better than 20%. In Ref. 1, it was concluded that in the energy region below 25 keV/u, the PSS (or CC-MO) method can provide an accuracy of the category (a) if the molecular-orbital basis contains about (3–4)q states (q being the ionic charge) with appropriate electron translational factors included in the basis functions. In the region $\sim$10–400 keV/u, the CC-AO method provides a $\pm$ 20% accuracy if the number of basis states is about $\sim$(5–6)q, or somewhat smaller if appropriate pseudostates are included. In the energy range above $\sim$500 keV/u, the CDW method is able to provide a $\pm$ 20% accuracy for the total cross section if it is applied separately to the first $\sim(q + 3)$ final states and the contribution from the higher states is accounted for by the n^{-3} Oppenheimer's rule.

The above conclusions about the accuracy of the three "bench-marking" methods also hold in the multielectron target case, provided the electronic states are accurately described and the reaction channels corresponding to simultaneous many-electron transitions or to multistep processes can be neglected. In assessing the accuracies of the calculations for particular reactions presented in Table 1, in addition to using Table 4 as a guide, we have paid special attention to the approximations made in the electron state description and to the influence of multielectron and multistep transition processes to the electron capture channel.

The accuracy of electron state description plays a particularly important role in cross-section calculations by the CC-MO, CC-AO, and CDW methods, since these have the intrinsic ability to produce highly accurate ($\pm$ 20%) cross-section data. A self-consistent method for generating electronic states (i.e., molecular or atomic orbitals) is deemed to

be a minimum requirement to assure that the electronic state representation does not introduce an uncertainty in the cross-section results of greater than 20%–30%. For helium, a variational wave function with at least three parameters is required to attain the same goal. In the two-state models (LZ, RZD, AM, AM-Res), the accuracy of the obtained results (within the model itself) is strongly influenced by the accuracy with which the coupling interaction is calculated. Criteria for assessing the accuracy of coupling-interaction calculations are available.[3] The accuracy of cross-section data calculated by the two-state models can be significantly affected by the neglect of the coupling with other possible reaction channels. An analysis of the reaction dynamics is needed for each of the collision pairs treated by a two-state model to assess the uncertainty in the results introduced by the neglected channels. (In most cases where two-state models were employed, the authors have already considered the applicability of the model.) Except at very large collision energies and/or for low-charged ions, the effects of the electronic structure of the projectile ion do not play a critical role in the calculations. If the collision energies are such that the ionic core electrons do not participate in the collision dynamics, the ion is usually described by an effective charge, determined from spectroscopic data. The aspects introduced in the accuracy assessment procedure by the structure of the projectile ion were analyzed in detail in Ref. 2.

The above discussion regarding the effects of electronic structure and collision dynamics on the accuracies of the methods presented in Table 4 remains valid also for the ion–ion charge exchange collisions. In almost all of these calculations, listed in Table 2, the Coulomb trajectory effects have been explicitly taken into account. (Exceptions are the calculations in Ref. 51). We note that these effects are small (in the total capture cross section) for energies well above the one corresponding to the cross-section maximum, but they may be very large in the energy region below the cross-section maximum. (For the quasiresonant reactions, the Coulomb repulsion of nuclei introduces a threshold.[27])

For the two-electron capture processes (listed in Tables 2b and 3), the correlation between the two active electrons plays a major role, particularly at low energies. An independent-particle model is not expected to be adequate even in the upper region of the energy range investigated in the present report ($\lesssim 1$ MeV/u) and may significantly degrade the accuracy in the calculation of single-particle transition probability attained by a highly accurate method, such as CDW.

For some of the methods listed in Table 4, the accuracy is left unspecified because of the lack of firm theoretical arguments. For these methods (VPS-Emp, BK-Emp, B1, B-B1, CPB), the accuracy of the cross-section calculations can be established only for specific reaction systems for which there are both accurate theoretical calculations and experimental data for comparisons. A similar approach of comparing relative accuracies can be used also for the calculations in which the uncertainty introduced in the results by the inadequate treatment of electronic structure (and neglected reaction channels) is difficult to assess directly.

For most of the methods with a stated accuracy in Table 4, the relative accuracy can be established from the reactions of He with He^{2+} for which large-base close-coupling calculations in the low- and intermediate-energy regions and CDW calculations in the high-energy region exist, together with reliable experimental data (see Figs. 1 and 18). The conclusions obtained from such a comparative analysis can then be extended to other reaction systems and checked (or corrected) on other less complex systems when experimental data exist (e.g., He + Li^{3+},C^{6+},N^{7+},O^{8+}, see Figs. 2, 7, 8, and 10, respectively).

It is obvious that such a procedure, even complemented by an analysis of the electronic structure and collisional dynamics effects on the accuracy, cannot pretend to produce critically evaluated cross-section data for the collision systems for which highly accurate theoretical calculations and reliable experimental data do not exist. However, even for such systems the adopted procedure provides a rough assessment of the accuracies of calculated cross sections.

5. Evaluated Cross-Section Data

The accuracy of the cross-section data for each analyzed charge exchange reaction listed in Tables 1–3 has been determined by employing the procedures described in the preceding section and is shown in the last column of the tables. Before going into the details of how these procedures have been applied to particular reactions, we note the following: The appearance of two symbols [(a,b), or (b,c), for example] in these tables means that the accuracy of the data is not uniform in the entire energy region in which they are calculated. The better accuracy is pertinent for that part of the energy region investigated in which the validity conditions of the method are better fulfilled. The data having an accuracy within a factor 2 or better (a, b, or c) are presented in Table 5 (for one-electron capture in ion–atom collisions), Table 6 (for one-and two-electron capture in ion–ion collisions), and Table 7 (for two-electron capture in ion–atom collisions). Some illustrative examples are presented in graphical form (Figs. 1–19). Experimental data, where available, are also shown in these figures and are indicated by a letter E after the reference number in the legend. In presenting the data in Tables 5–7 or in the figures, we have adopted the following criteria:

From all available calculations using the same method, only those with highest accuracy are presented;

If the calculations are extended outside the region of validity of the applied method, only the part which conforms with the validity region is presented;

The VPS-Emp and BK-Emp data listed in Table 1 are presented in their entirety since they contain a fitting parameter to conform with experimental data;

Graphical presentation is made of data for those reactions for which more than two calculations exist and/or there are reliable experimental data for comparison (with a few exceptions);

We now give some details on the application of assessment procedures to particular reaction cross-section calculations, or to entire classes of them.

5.1. Single-Electron Capture Reactions

a. He Target

The availability of reliable experimental data for the He^{2+} + He single capture cross section in the entire energy region 1–1000 keV/u (see Fig. 1, and the references quoted there), and the simple structure of this system, make the assessment of the accuracies of theoretical calculations for this reaction a relatively easy task. In the energy region from 3 to 34 keV/u, there are 16-MO-states close-coupling calculations,[5] for which the molecular orbitals (MO) were determined by the OEDM code (see Ref. 5 for details). The 16-MO basis can be considered as sufficient for this two-electron system to account for all the dominantly interacting states in the energy region considered. Since the two-electron capture channel has also been included in the calculations, and the ionization channel is small at these low energies, one can expect that the obtained results have an accuracy of at least $\pm$ 50%. The comparison with the experimental data of Refs. 62 and 67 confirm this conclusion. In the region from 25 to 750 keV/u, there are CDW calculations[24] with a 35-term configuration interaction (CI) wave function for the initial state. In the region above 300 keV/u (for this particular system), the CDW method is expected to give an accuracy within $\pm$ 20%. The accuracy of the above-mentioned CI wave function is certainly well within these limits. Therefore, one can ascribe an accuracy (a) to these calculations in the region above 300 keV/u. As can be seen from Fig. 1, the CDW calculation of Ref. 23, with a three-parameter variational wave function for the initial state, gives essentially the same accuracy. The agreement of experimental data from Refs. 64–66 with the CDW calculations above 200 keV/u is within 10%–40%, but agreement among the experimental results themselves is also within these limits. In the region from 30 to 300 keV/u the 3-AO state close-coupling calculations, supplemented by taking into account six other states through a pertubational treatment,[29] give an accuracy well within $\pm$ 50%. The experimental data in the region 30–200 keV/u are dispersed within the same accuracy limits (see Fig. 1). The three calculations mentioned have been taken as standards (with their absolutely determined accuracies) against which we have determined the accuracies of all other calculations for the He^{2+} + He single-electron capture reaction.

In assessing the accuracy of different calculations for He-fully (or highly) stripped ion systems one should consider that, although the number of active electrons remains the same as in the He^{2+} + He system, any close-coupled calculation would require a much larger basis of states (roughly proportional to q). The reason is that electron capture may now go into a group of excited levels of the projectile, the number of which increases with increasing q and the energy (up to $\sim$ 50 keV/u). For sufficiently high values of q ($q \gtrsim 8$), two-electron capture and simultaneous capture and ionization become important reaction channels, which are coupled with the single-electron capture. (Capture of two electrons at low energies leads to creation of a double excited state which decays rapidly by ejection of one of the electrons into the continuum, therefore changing the projectile charge by one unit only.)

For the He + Li^{3+} system the above channel-coupling problem is not expected to be pronounced, and calculations have been performed by UDWA[35] in the range 10–1000 keV/u and CTMC[31] in the range 100–200 keV/u. In the regions of their validity, both of these methods are expected to give an accuracy of $\pm$ 50% (see Table 4), and description of the helium target within an independent particle model (with $Z_{eff} = 1.69$) is not expected to degrade considerably the accuracy of the results in the energy region above $\sim$ 50 keV/u. The experimental results of Refs. 68–70, shown in Fig. 2, confirm this assessment. For the CTMC method, the above conclusion is experimentally confirmed also on the He + B^{5+}, C^{6+}, N^{7+}, and O^{8+} reaction systems, as shown in Figs. 6, 7, 8, and 10, respectively. The results of Ref. 20, plotted in these figures and in Fig. 11 for He + F^{9+}, as well as those of Ref. 32 for He + Si^{14+} in Fig. 12, have a semiempirical origin (empirically normalized B1). The VPS-Emp results of Ref. 40, plotted in Figs. 9 and 10 (for He + O^{6+} and O^{8+}, respectively) contain a normalization factor of 1/3, which also has an empirical origin.

For the reactions of He with incompletely stripped ions, the assessment procedure becomes more difficult and less reliable (correspondingly, the uncertainty limits larger). The uncertainties of the assessment procedure are, of course, somewhat reduced for the reactions for which experimental data exist. PSS calculations have been performed for He + B^{3+} (Ref. 7) and He + C^{4+} (Ref. 6) with four- and five-MO bases. In the first instance, the basis, although small, accounts for the major couplings in the system and an accuracy within $\pm$ 50% can be expected. The comparison with the experimental data (Refs. 71–73) shows an agreement of this degree of accuracy (see Fig. 5). For the second reaction, however, the five-state MO basis seems to be insufficient, due to the strong coupling of the one- and two-electron capture channels (see Fig. 19 for the value of two-electron capture cross section). Therefore an accuracy of $\pm$ 40%–100% (b,c) has been ascribed to these calculations, which conforms with the experimental data.[92]

For the other reaction systems of this category, the cross sections have been performed by less accurate models (LZ, RF, DM, BK-Eik), and if there were no experimental data to compare with, we have ascribed to the corresponding cross sections (in the region of validity of the models) an accuracy in accordance with Table 4. We note that the cross sections calculated by the decay model (DM) refer to the sum of single-, double-, etc., electron capture cross sections. For the summed cross section (σ^*_{tot}), this model provides a factor of 2 accuracy or even better (see, e.g., Ref. 3, for examples). Therefore, for the DM cross-section calculations presented in Table 1, we have ascribed a (b,c) accuracy.

b. Alkali Atom Targets

For the simplest three-electron system, Li + He^{2+}, extensive close-coupling calculations have been performed in the region 0.05–2 keV/u by the PSS method using 12 MO states,[8] and in the region 0.1–20 keV/u using the CC-AO method with 40 states.[18] For the region $\sim$ 10–400 keV/u, CTMC calculations have been performed by using the independent-electron, independent-shell model with an effective

core charge for each shell.[8,44] Experimental data for this reaction are available in the region above 0.1 keV/u (Refs. 80–82 and 92). The CTMC cross sections (summed over the K and L shell) are consistent with the experimental data within a 50% accuracy (see Fig. 15). In the energy region 2–4 keV/u, the experimental data of Refs. 80 and 92 are inconsistent: Those of Ref. 80 show a decrease with decreasing energy, while the data of Ref. 92 are flat in this region and begin to decrease only at about 0.8 keV/u. The difference between the two experimental cross sections at 2 keV/u is a factor of 2.

The 40-state CC-AO calculations[18] agree with the experimental data of Ref. 90 within $\pm 25\%$ down to $E \simeq 0.25$ keV/u and to within 30%–40% in the range 0.1–0.2 keV/u (see Fig. 15). In contrast to this, the 12-state CC-MO calculations[8] follow the trend of the experimental data from Ref. 80 (these data are not shown in Fig. 15 below the 4 keV/u energy), and at ~ 0.1 keV/u disagree with CC-AO calculations and the data of Ref. 90 by a factor of about 5. We gave priority to the 40-state CC-AO calculations over the 12-state PSS calculations on the basis of the following arguments: (i) the basis of the CC-AO calculation was substantially larger than that of the PSS calculations and was supplemented by a set of united-atom pseudostates to describe the electronic motion at small internuclear distances; (ii) the experimental data of Ref. 82 in the region 3.5–5 keV/u exhibit a trend which can be smoothly connected with the behavior of the experimental cross section of Ref. 90 below 1 keV/u; and (iii) they are consistent with the two-state CC-AO calculations[43] in the region 2.5–5 keV/u, where the maximum of the cross section lies. [The reaction $Li + He^{2+} \rightarrow Li^+ + He^+ (n = 3)$ is quasiresonant and a two-state approximation well describes the process in the energy region around its maximum.]

For all other electron capture reactions of Li, as well as for those of other alkali target atoms, only σ^*_{tot} cross sections have been calculated at $E = 1.32$ keV/u by using the decay model. As discussed earlier, we ascribe an accuracy between 30% and 100% to these data.

c. Inert Gas Atom Targets (Other Than Helium)

In the low-energy region, most of the electron capture cross-section calculations for inert gas atom targets other than helium have been performed by the DM method at selected collision energies (see Table 1). In a few cases, there are also low-energy calculations performed within the RF or LZ models (Refs. 10 and 39). The accuracy of the latter is low [(c) or (d)] as assessed on the basis of comparison with experimental data (Ref. 10 and 39), the employed two-state coupling matrix elements, and of neglected reaction channels.

At higher energies, electron capture from the inner shells starts to play an important role for these target systems. The maximum of the cross section for electron capture from a particular subshell with a mean binding energy $\overline{E}^{(i)}_{b,s}$ takes place approximately at a collision energy[46]

$$E \sim |\overline{E}^{(i)}_{b,s} - E^f_b|,$$

where E^f_b is the binding energy of the electron in its final state. The independent-shell (or subshell) model is usually assumed to be acceptable in the high-energy region, although this assumption may introduce considerable uncertainty in the calculations at energies where the contributions to the cross section for two shells (or subshells) are comparable. In the medium to high-energy region, VPS-Emp cross sections summed over the electronic shells of the target have been performed[40] for $Ne + Xe^{q+}$ $(q = 2,4,8,10)$ and $Ar + F^{7+}$, and their accuracy, although unspecified on theoretical grounds, may lie within a factor of 2 or so, as suggested by the comparison with experimental data. (This assessment has not been entered in Table 1.)

Most of the calculations for these target atoms, however, have been done for K- and L-shell electron capture. For $Ne + He^{2+}$ and $Ne + Li^{3+}$, CC-AO calculations with a 48 Hartree–Fock state basis have been reported in Ref. 15 at energies from 400 to 4000 keV/u. Since the coupling between the K- and L- shell capture channels has been adequately accounted for in the calculations, and since the target electronic states have been described sufficiently well, we have ascribed an accuracy (a) or (b) to these large-basis calculations. In the region above 1000 keV/u, this assessment has also been supplemented by comparison with experimental data for the $Ne + Li^{3+}$ case[83] (see Fig. 16). Similar large-basis CC-AO calculations, including pseudostates to describe the coupling with the continuum, have also been performed for the $Ar + He^{2+}$, C^{4+}, and C^{6+} systems[16] in the region 1–9 MeV/u. For the same reasons as in the $Ne + He^{2+}$, Li^{3+} cases, we have ascribed an (a) or (b) accuracy to these cross sections. For Ne, Ar, and Kr atoms, colliding with fully stripped ions C^{6+}, N^{7+}, F^{9+}, Cl^{17+}, K-shell to K-shell electron transfer calculations have been performed by using a two-state CC-AO method[45] in the energy region above 1 MeV/u. An independent-electron model, with adequately chosen effective core charge to account for the screening effects, can provide a factor of 2 accuracy for such calculations in this energy region, as confirmed by the experiments (see, e.g., Ref. 45). Therefore, an accuracy (b) or (c) has been adopted for these calculations, except where comparison with reliable experiments suggest otherwise (see Table 1). For the other collision systems of this class, similar arguments were used in assessing the accuracy of theoretical calculations.

d. Other Target Atoms

For $Ti + He^{2+}$ (Ref. 16) and $Cu + He^{2+}, C^{6+}, O^{8+}$ (Ref. 17), large-basis (+ pseudostates) CC-AO calculations have been performed in the energy range 2–8 MeV/u (for Ti) and at 6.07 MeV/u (for Cu). The calculations are of the same type as those for $Ne + Li^{3+}$, $Ar + He^{2+}$, and $Ar + C^{6+}$ discussed in Sec. 5.1.c, and on the basis of the same arguments we have ascribed to them an (a) or (b) accuracy. Two-state CC-AO calculations for $Cu + Si^{14+}$, S^{16+}, and Cl^{17+} for K-shell–K-shell electron transfer at selected energies have been performed in Ref. 19. Comparison with available experimental data (see Refs. 19 and 45) suggests a (b) accuracy for S^{16+} and Cl^{17+} impact and a (d) accuracy for the Si^{14+} impact.

Calculations for $C + He^{2+}$, Li^{3+} have been done in the energy range ~ 0.8–3 MeV/u by the BK-Eik method,[34] with

an effective target core charge. Although the accuracy of this method cannot be estimated on pure theoretical grounds, the comparison with numerous experimental data for different systems suggests that it can provide an accuracy within the (b) or (c) categories. Our assessment (b), given in Table 1, was determined from comparison with experimental data (see Ref. 37).

For other collisional systems, the cross-section calculations have been performed by methods for which the assessment procedure has been discussed in the previous subsections.

5.2. Ion–Ion Charge Exchange Reactions

As we have mentioned in Sec. 4, the dynamical aspects of ion–ion charge exchange collision processes remain the same as in the ion–atom collisions, except that Coulomb trajectories have to be used for description of nuclear motion (in the semiclassical approximation of the collision process). In the total cross-section calculations at high energies, the Coulomb trajectory effects can be neglected. However, these effects significantly affect the cross-section results in the low-energy region (around and below the cross section maximum). Except in Ref. 51, in all other calculations of ion–ion charge exchange cross sections, the Coulomb trajectory effects have explicitly been included. Therefore, the assessment of the accuracies of the calculations presented in Table 2 has been done on the basis of Table 4 and other considerations regarding the employed coupling interactions, influence of different neglected reaction channels, etc. No experimental data exist for these reactions. The low-energy electron capture cross sections for the one-electron reaction systems from $He^+ + He^{2+}$ to $O^{7+} + O^{8+}$ (Ref. 25) have been performed by using the two-state asymptotic theory for the resonant charge transfer process with an asymptotically correct expression for the coupling interaction. Previous experience with cross-section calculations by this method for ion–atom reactions suggests that the accuracy of obtained results is well within a factor of 2. Therefore, we assign a (b,c) accuracy to the calculations of Ref. 25. On the basis of the same arguments we have assessed the accuracy of resonant two-electron capture cross sections in Table 2b. (With increasing ionic charge states, the two-state approximation becomes increasingly better for the resonant electron transfer between low-lying states.)

The accuracy of the calculations of Ref. 27 for the quasiresonant one-electron capture reactions $He^{2+} + O^{2+}$, $C^{2+} + B^+$, $N^{3+} + C^{2+}$,..., $N^{6+} + F^{5+}$ has been determined by arguments similar to those used above for resonant reactions. The analysis of the structure of reaction systems has shown that in the considered energy range the use of the two-state approximation is justifiable.

The accuracy of the CDW calculations (Refs. 24 and 29) for the single-electron systems presented in Table 2 has been determined on the basis of Table 4 and for the CTMC calculations (Ref. 53) has been estimated by the author of the calculations.

In Ref. 51, the only case where Coulomb trajectory effects have not been included in the calculations ($O^+ + C^{6+}$,..., $O^{3+} + O^{8+}$, see Table 2), we have found that the calculated cross section (for the two selected energies) lie in the region of the cross-section maximum (usually broad for quasiresonant reactions). On the basis of general accuracy of the LZ method and neglected Coulomb trajectory effects (not large in the region of the cross-section maxium), we have ascribed an accuracy (c) or (d) for these cross sections.

5.3. Ion–Atom Two-Electron Capture Reactions

Numerous cross-section calculations have been performed for the double-electron capture in the $He + He^{2+}$ system in the region from 0.1 to ~500 keV/u using different methods. In the energy region above ~2 keV/u, there also exist experimental data for the process (see Fig. 18). In the low-energy region (~3–33 keV/u), PSS calculations with a 16-state MO basis have been performed for this system (Ref. 5). Considering the accuracy of the basis functions (see the discussion for the $He + He^{2+}$ single-electron capture) and the size of the basis, one can determine that the accuracy of the calculations is well within $\pm 40\%$. The experimental data of Refs. 62, 63, 89, and 91 in this region are in disagreement to within the same uncertainty. In the intermediate energy range, ~1–375 keV/u, three-state CC-AO calculations (plus six other states included perturbationally) have been performed for this system,[29] and they are within a 50% agreement with the experiment in the region above 100 keV/u, and less accurate at lower energies. The CDW method has also been used[58] to calculate the double-capture cross section in this system (energy range 125–350 keV/u). However, the use of an independent-particle model (multiplication of single-electron probabilities) degrades the accuracy of the method to a (b) or (c) category (see Fig. 18).

For the $He + C^{4+}$ system, the two-electron capture channel below ~2 keV/u dominates over the one-electron capture.[92] The four-state PSS calculations[6] and the LZ calculations with a correct coupling interaction[30] agree with the experimental data to within 30% as shown in Fig. 19. Three-state CC-AO calculations for K-shell two-electron capture in $Ne + N^{7+}$, O^{8+}, F^{9+} systems have been performed[57] in the energy range of ~1–5 keV/u. Although the coupling with the L-shell electrons has been included to some extent in these calculations, we expect that their accuracy cannot be better than category (c). CDW calculations have been performed in the independent-electron model also for the $Ar + F^{9+}$ system.[58] On the basis of the same arguments used in the $He + He^{2+}$ case, we have assessed the accuracy of these calculations to be within a factor of 2.

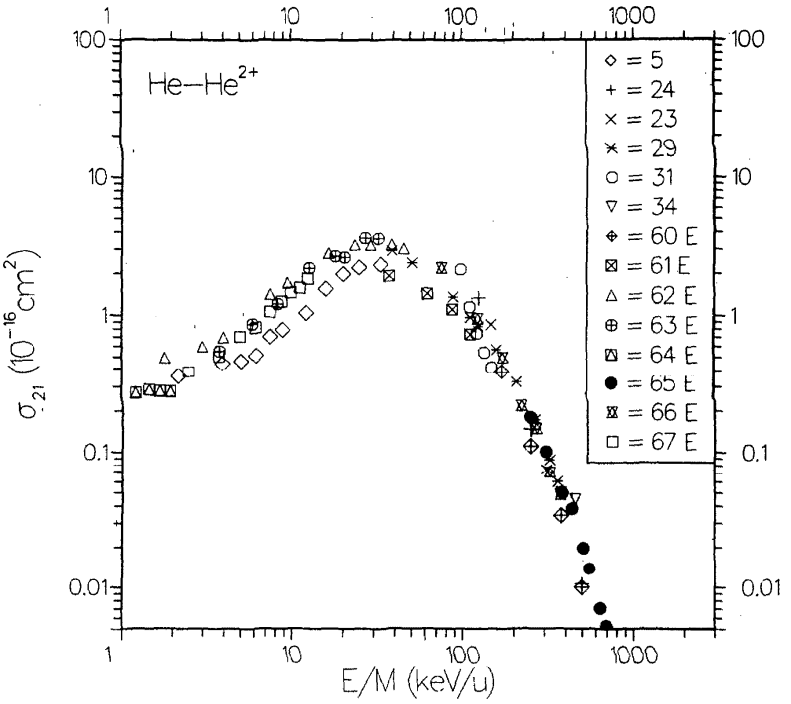

FIG. 1. Cross sections for single-electron capture in He–He^{2+} collisions.

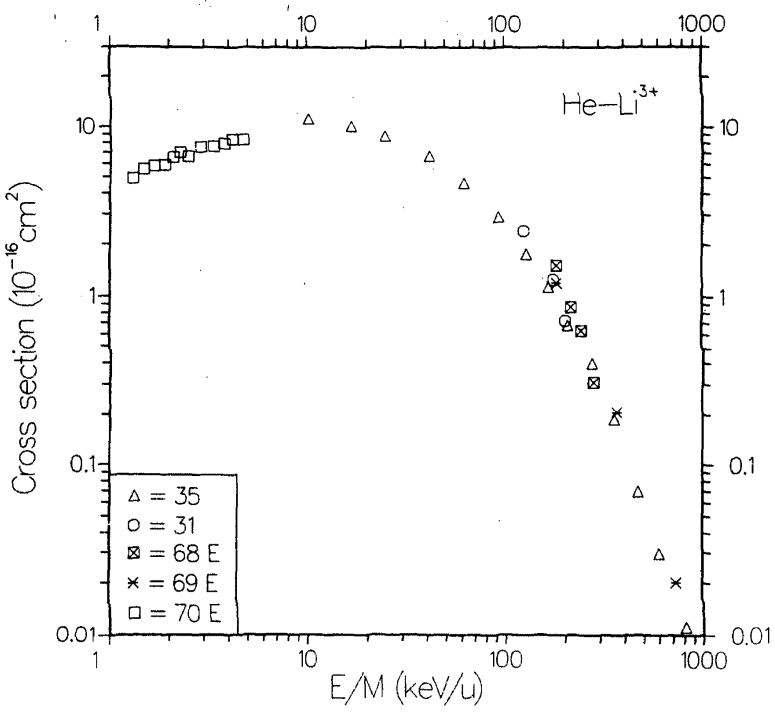

FIG. 2. Charge exchange cross sections for He–Li^{3+} collisions.

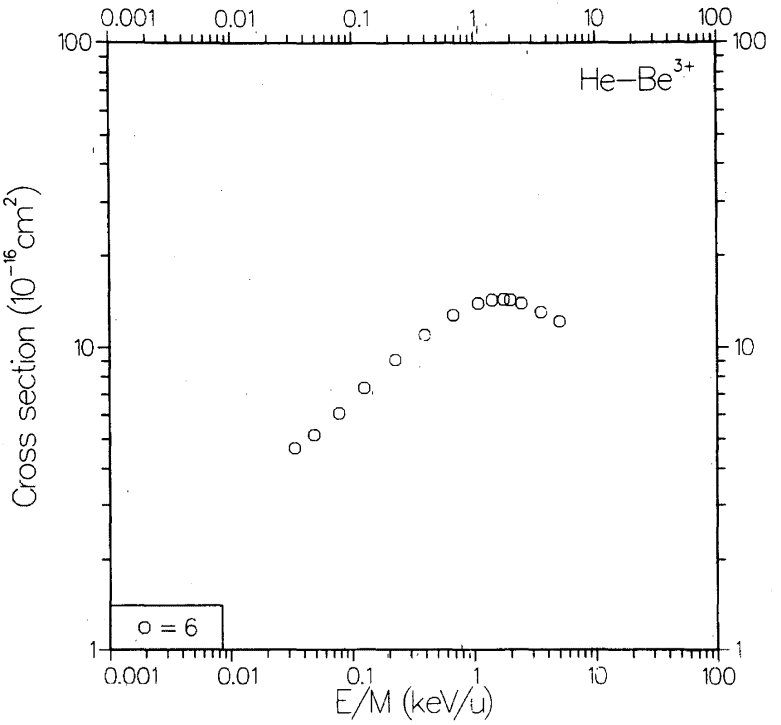

FIG. 3. Charge exchange cross sections for He–Be^{3+} collisions.

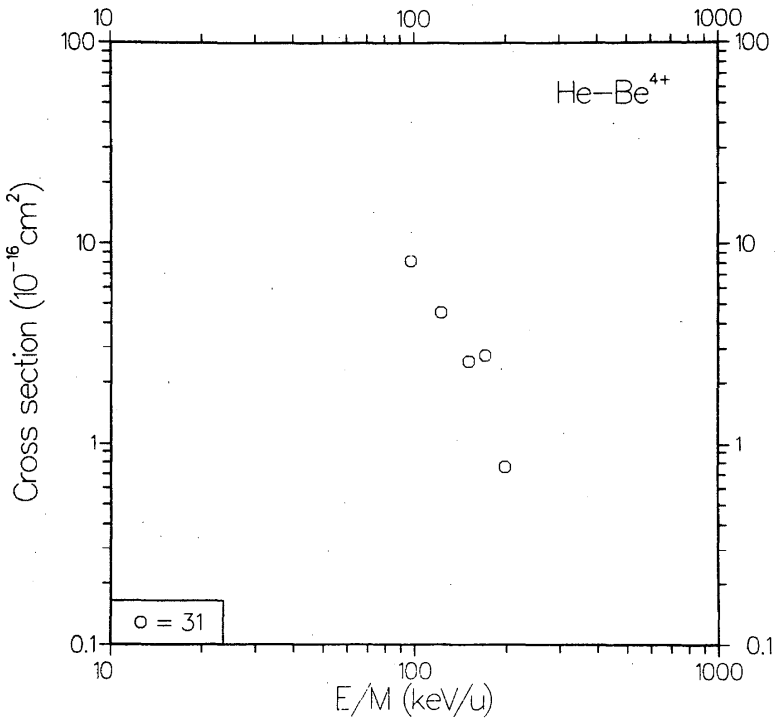

FIG. 4. Charge exchange cross sections for He–Be^{4+} collisions.

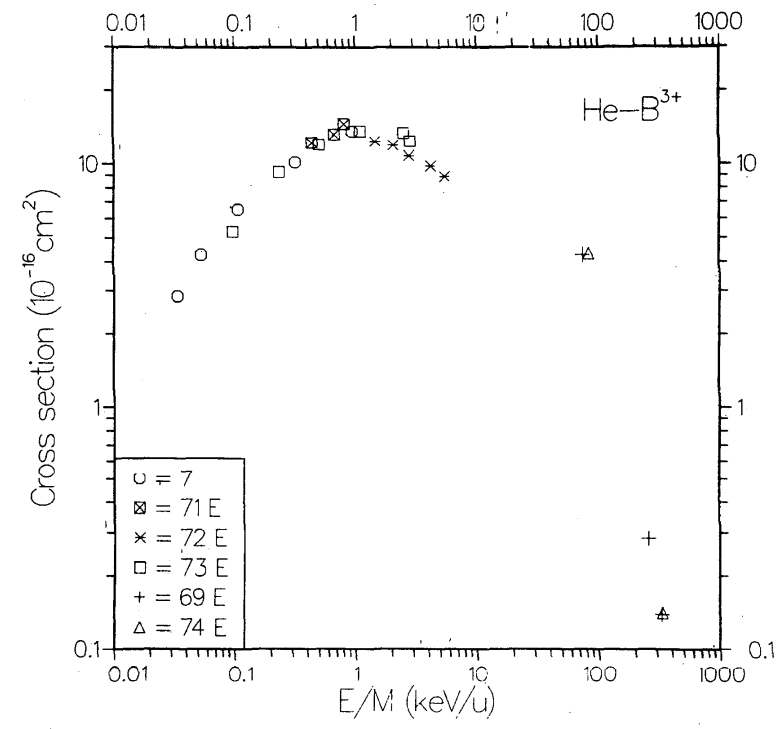

FIG. 5. Cross sections for charge exchange in He–B^{3+} collisions.

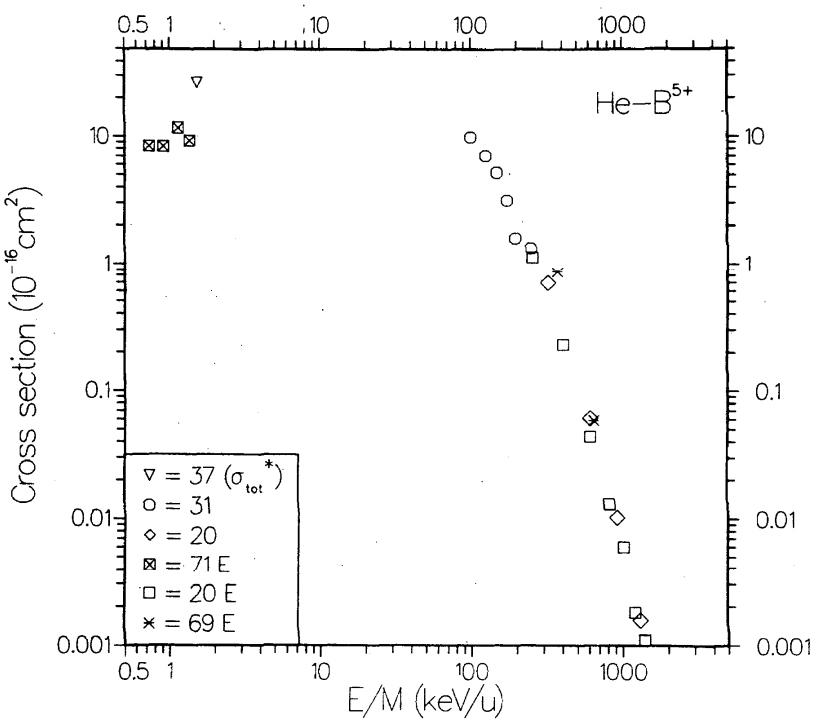

FIG. 6. Charge transfer cross sections for He–B^{5+} collisions. The notation σ_{tot}^* indicates that the contribution of one-, two-, and more-electron capture is included in the cross section.

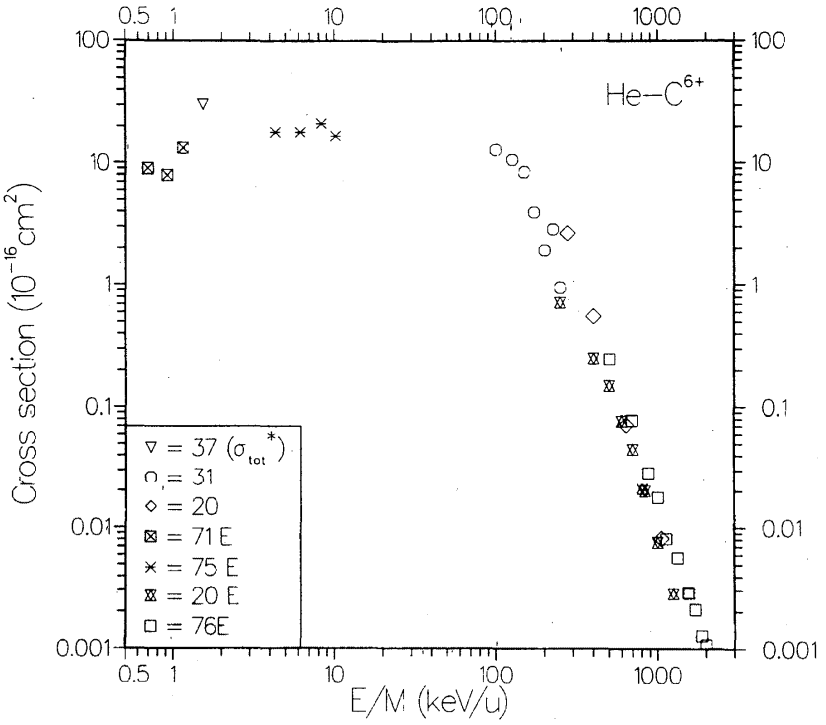

FIG. 7. Charge exchange cross sections for $He–C^{6+}$ collisions. See caption to Fig. 6 for definition of σ^*_{tot}.

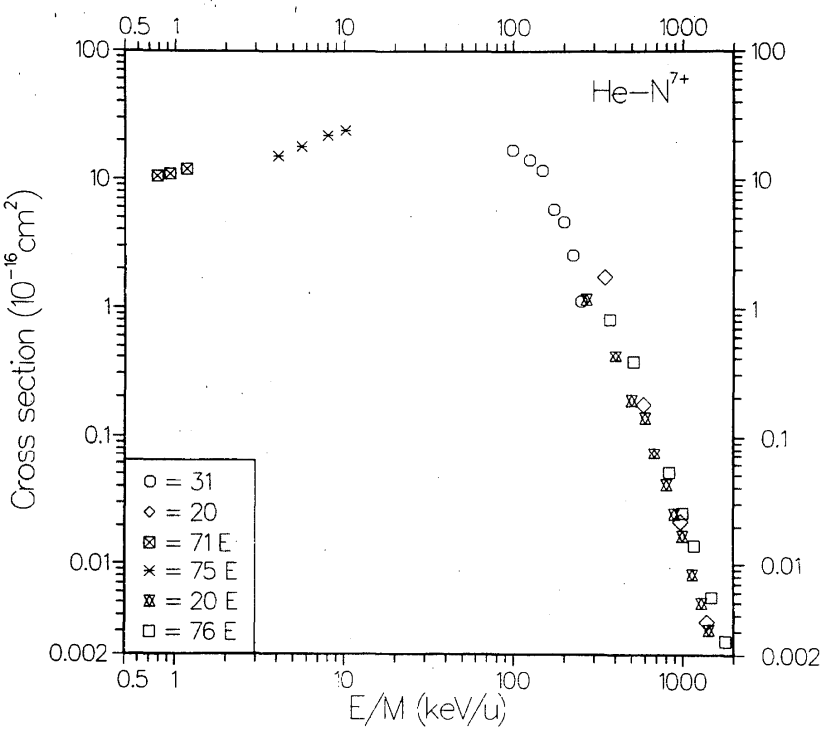

FIG. 8. Charge transfer cross sections for $He–N^{7+}$ collisions.

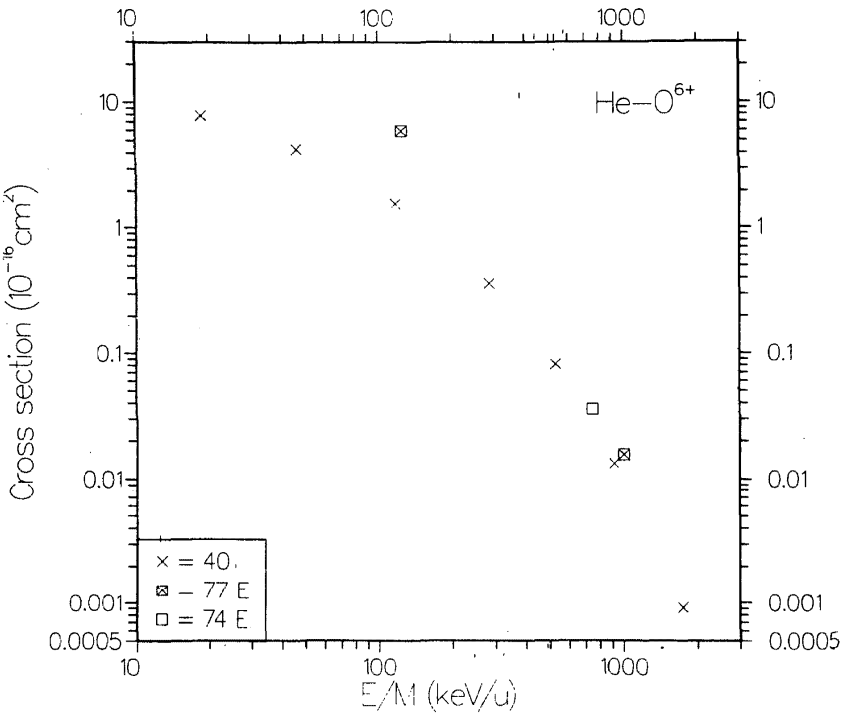

FIG. 9. Cross sections for charge transfer in $He–O^{6+}$ collisions.

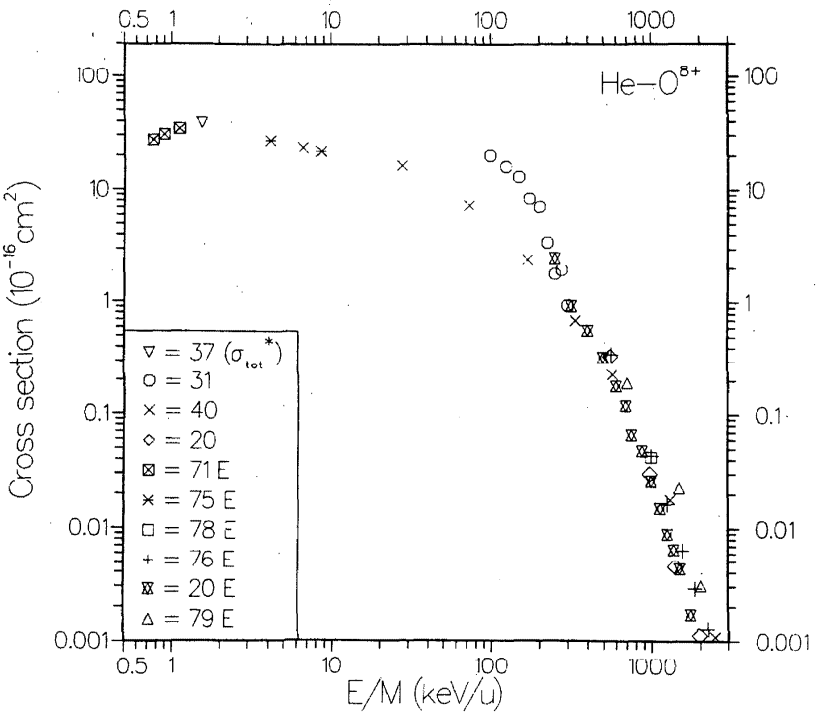

FIG. 10. Charge exchange cross sections for $He–O^{8+}$ collisions. σ^*_{tot} is defined in the caption to Fig. 6.

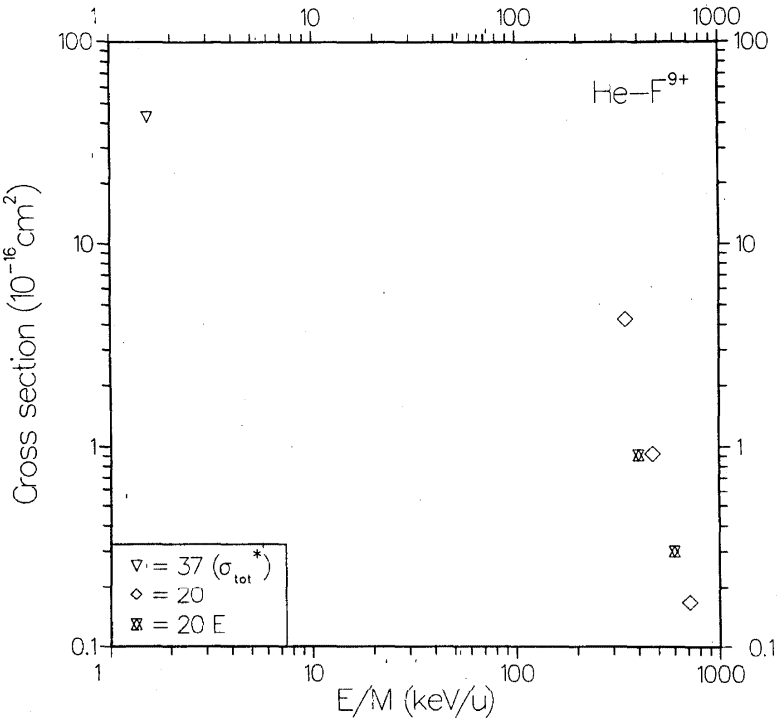

FIG. 11. Cross sections for charge transfer in He–F^{9+} collisions. See caption to Fig. 6 for definition of σ^*_{tot}.

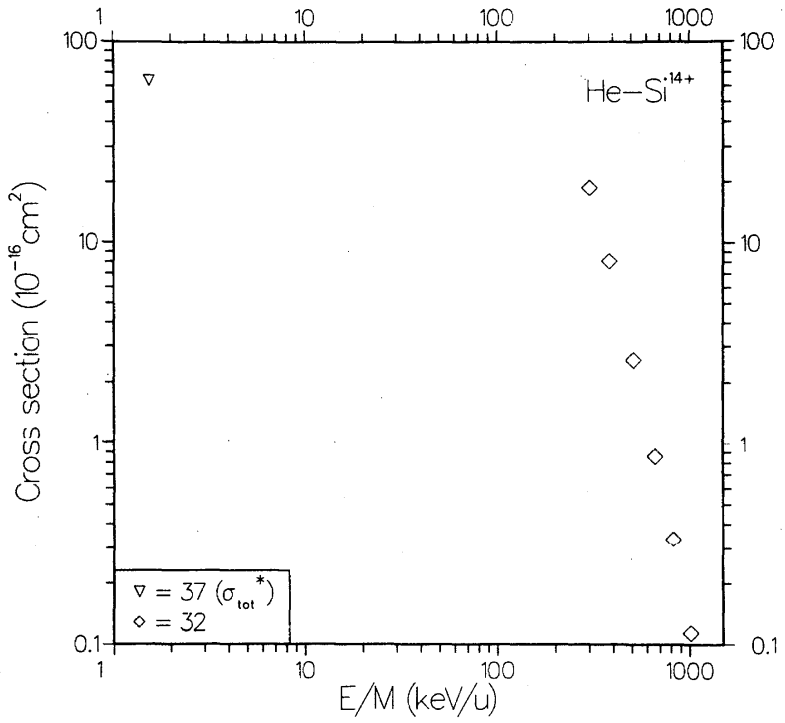

FIG. 12. Cross sections for charge transfer in He–Si^{14+} collisions. See caption to Fig. 6 for definition of σ^*_{tot}.

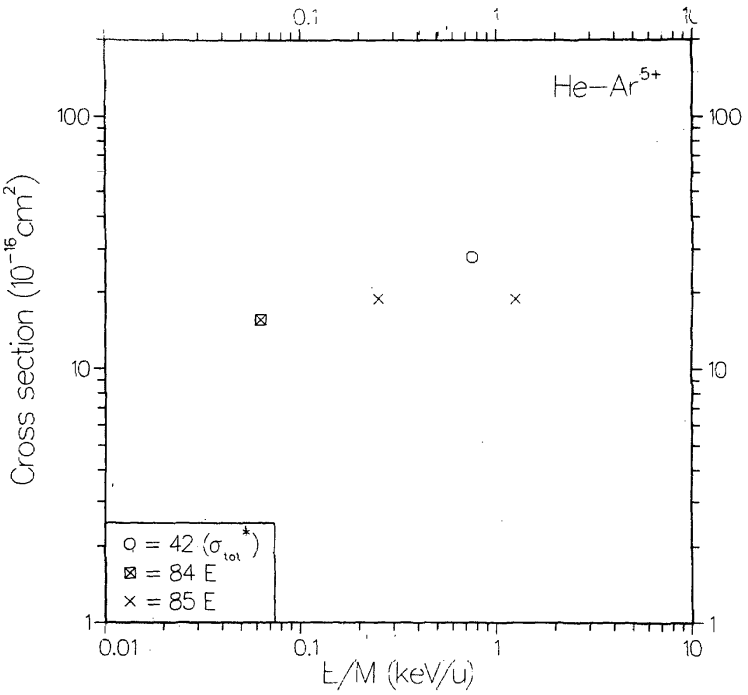

FIG. 13. Charge exchange cross sections for He–Ar^{5+} collisions.

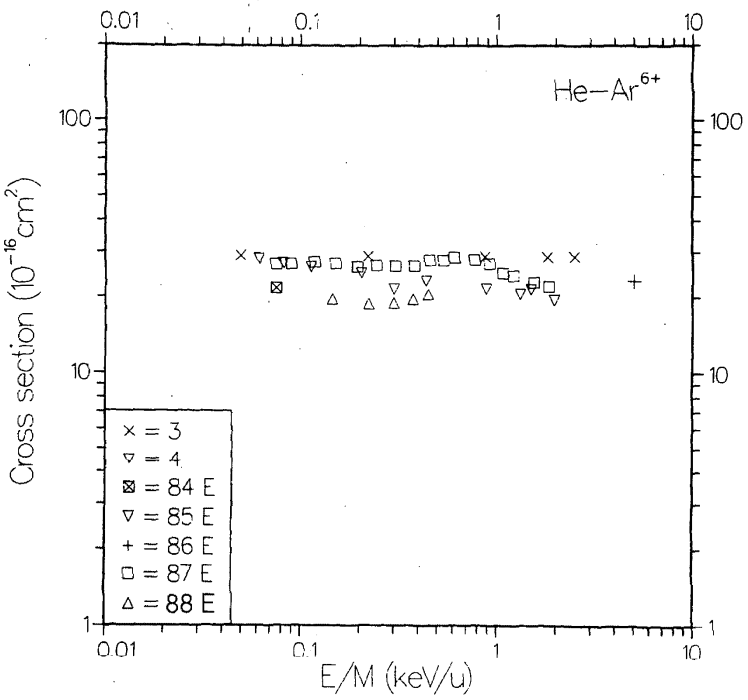

FIG. 14. Charge exchange cross sections for He–Ar^{6+} collisions.

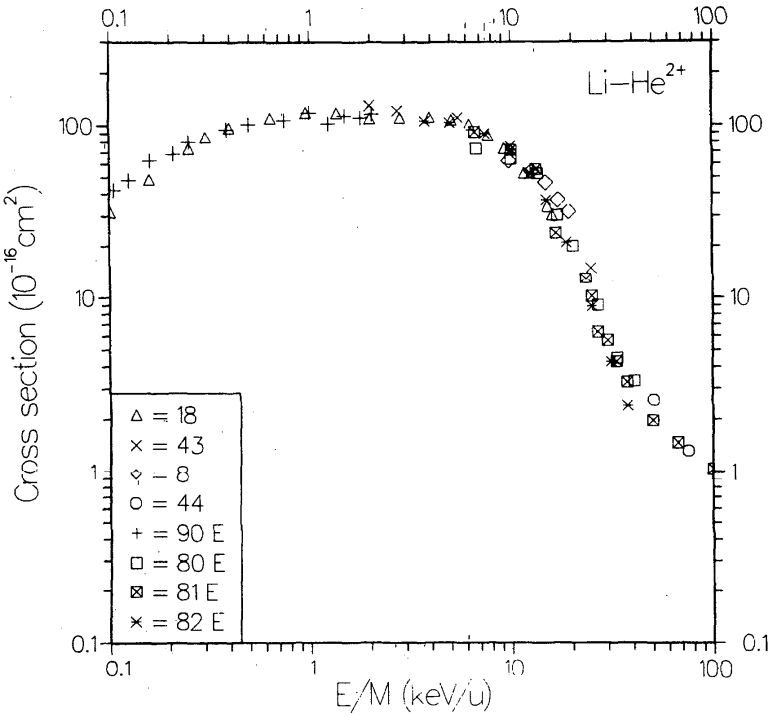

FIG. 15. Cross sections for charge transfer in Li–He^{2+} collisions.

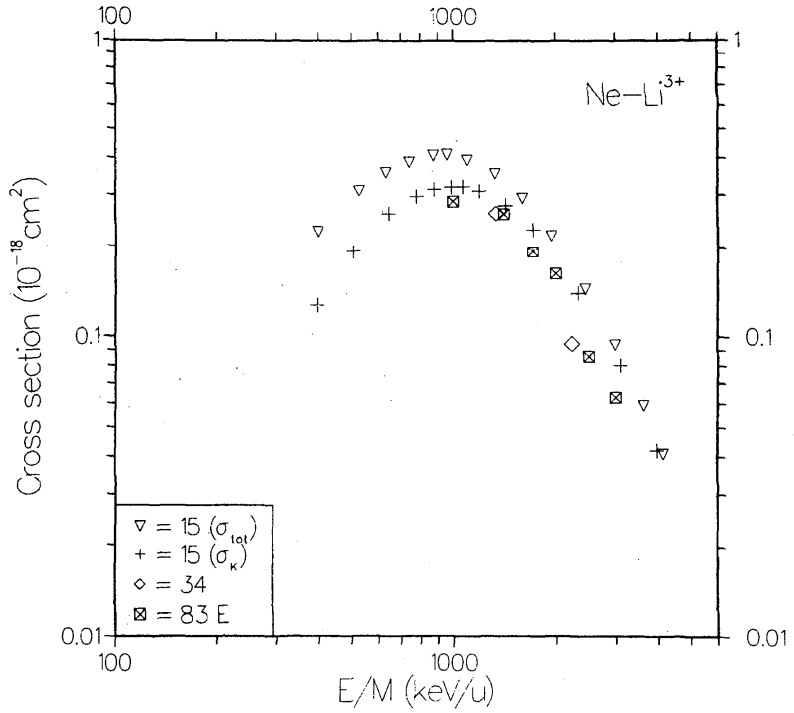

FIG. 16. Cross sections for charge transfer in Ne Li^{3+} collisions.

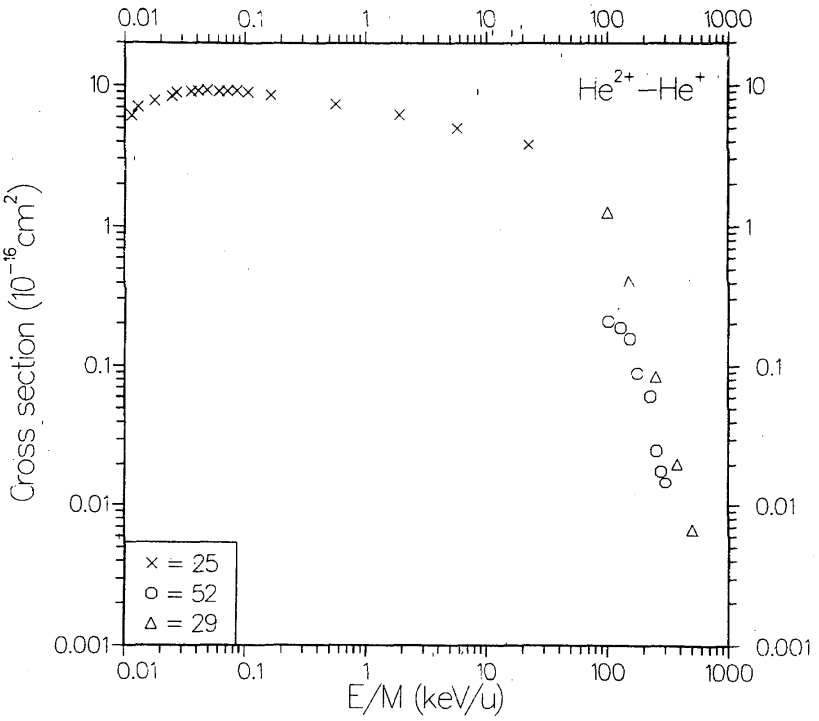

FIG. 17. Charge transfer cross sections for He^{2+}–He^{+} collisions.

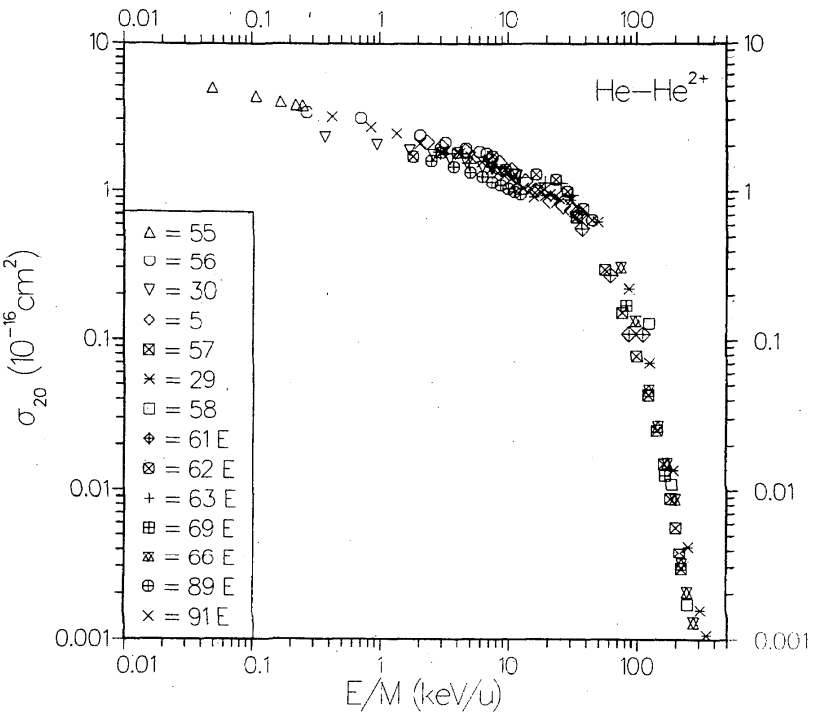

FIG. 18. Cross sections for double-electron capture in He–He^{2+} collisions.

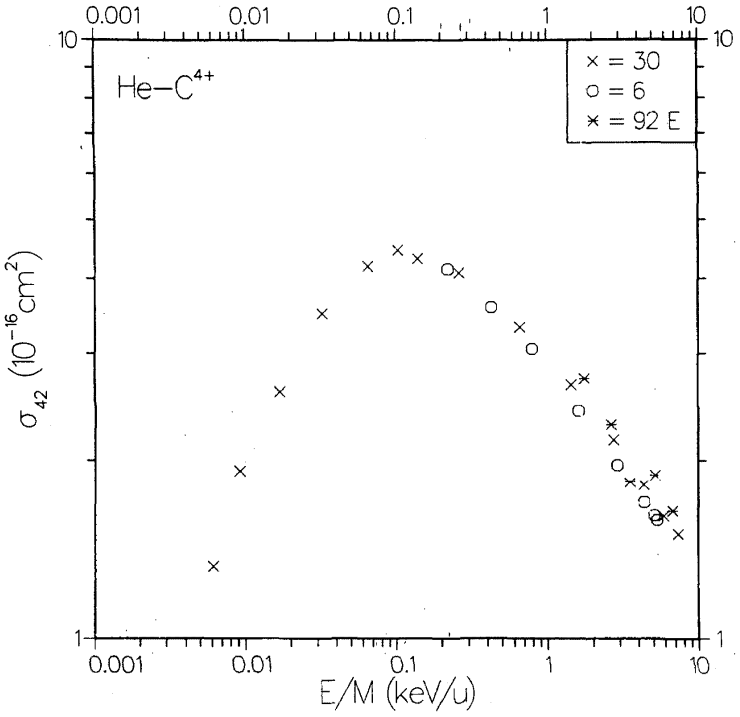

FIG. 19. Cross sections for double-electron capture in $He–C^{4+}$ collisions.

Table 1. Sources of theoretical data for charge transfer between atoms ($Z \geq 2$) and ions ($q \geq 2$)

Reference	Target Atomic Species	Projectile Ionic Species	Ionic Charge State	Energy Range (keV/u)	Method and Comments[a]	Accuracy
5	He	He	+02	3-34	PSS (16 states)	(a,b)
29	He	He	+02	1.25-375	CC-AO + perturb. method 9 states, 3 strongly coupled	(c) E < 25 (b) 25 < E < 100 (a) E > 100
31	He	He	+02	100-150	CTMC, Z_{eff}	(b)
32	He	He	+02	500-2000	BK-Emp	---
33	He	He	+02	16-250	B-B1 (σ_{1s-1s}) Independent electron model	(b,c)
34	He	He	+02	54-2000	BK-Eik, Z_{eff}	(c)
22	He	He	+02	6-750	CDW, 2 param. var. w.f.	(b,a)
24	He	He	+02	25-750	CDW (σ^{*}_{tot}) 35 term CI wave function	(a)
23	He	He	+02	25-2500	CDW, 3 param. var. w.f.	(a)
35	He	Li	+03	10-1000	UDWA, Z_{eff}	(b)
31	He	Li	+03	100-200	CTMC, Z_{eff}	(b)
6	He	Be	+03	0.03-5	PSS (4 states)	(a,b)
36	He	Be	+03	0.006-5.5	LZ	(c)
31	He	Be	+04	100-200	CTMC, Z_{eff}	(b)
7	He	B	+03	0.03-5	PSS (4 states)	(a,b)
37	He	B	+05	1.5	DM, σ_{tot}^{*}	(b)
31	He	B	+05	100-250	CTMC, Z_{eff}	(b)
20	He	B	+05	300-2400	BK-Emp	---
38	He	C	+02	---	$k_T^{\#}$	---
6	He	C	+04	0.2-5.23	PSS (5 states)	(b,c)
37	He	C	+06	1.5	DM, σ_{tot}^{*}	(b,c)
31	He	C	+06	100-250	CTMC, Z_{eff}	(b)
20	He	C	+06	300-2700	BK-Emp	---
39	He	N	+02	3-16	RF, stat. average	(c)
37	He	N	+07	1.5	DM, σ_{tot}^{*}	(b,c)
31	He	N	+07	100-250	CTMC, Z_{eff}	(b)
20	He	N	+07	300-2600	BK-Emp	---
10	He	O	+02	2-14	LZ; RF stat. average	(c)
40	He	O	+03	6-4000	VPS-Emp	---
40	He	O	+06	6-4700	VPS-Emp	---
37	He	O	+08	1.5	DM, σ_{tot}^{*}	(b,c)
31	He	O	+08	100-300	CTMC, Z_{eff}	(b)
40	He	O	+08	6-5600	VPS-Emp	---
20	He	O	+08	300-2600	BK-Emp	---
41	He	O	+08	285	BK-Eik, $\sigma_{n\ell}$	(b)
37	He	F	+09	1.5	DM, σ_{tot}^{*}	(b,c)
20	He	F	+09	300-2500	BK-Emp	---
42	He	Ne	+10	0.76	DM, σ_{tot}^{*}	(b,c)
37	He	Ne	+10	1.5	DM, σ_{tot}^{*}	(b,c)
37	He	Na	+11	1.5		
37	He	Mg	+12	1.5	DM, σ_{tot}^{*}	(b,c)
59	He	Al	+13	1.5		
37	He	Si	+14	1.5	DM, σ_{tot}^{*}	(b,c)
32	He	Si	+14	300-2000	BK-Emp	---

Table 1. Sources of theoretical data for charge transfer between atoms ($Z \geq 2$) and ions ($q \geq 2$) (cont'd.)

Reference	Target Atomic Species	Projectile Ionic Species	Ionic Charge State	Energy Range (keV/u)	Method and Comments[a]	Accuracy
37	He	P	+15	1.5	DM, σ_{tot}^*	(b,c)
37	He	S	+16	1.5	DM, σ_{tot}^*	(b,c)
37	He	Cℓ	+17	1.5	DM, σ_{tot}^*	(b,c)
42	He	Ar	+03	0.75	DM, σ_{tot}^*	(b,c)
42	He	Ar	+04	0.75	DM, σ_{tot}^*	(b,c)
42	He	Ar	+05	0.75	DM, σ_{tot}^*	(b,c)
42	He	Ar	+06	0.6-3.4	DM, σ_{tot}^*	(b,c)
9	He	Ar	+06	0.02-0.6	CC-MO (2 states) LZ for (3d) $\sigma_{n\ell}$ ($n\ell$ = 4s,4p,3d)	(b,c)
3	He	Ar	+06	0.05-25	classical model	
4	He	Ar	+06	1.32-0.06	DM	(b,c)
42	He	Ar	+07	0.75	DM, σ_{tot}^*	(b,c)
42	He	Ar	+08	0.75	DM, σ_{tot}^*	(b,c)
42	He	Ar	+09	0.75	DM, σ_{tot}^*	(b,c)
37	He	Ar	+18	1.5	DM, σ_{tot}^*	(b,c)
37	He	K	+19	1.5	DM, σ_{tot}^*	(b,c)
37	He	Ca	+20	1.5	DM, σ_{tot}^*	(b,c)
37	He	Sc	+21	1.5	DM, σ_{tot}^*	(b,c)
37	He	Ti	+22	1.5	DM, σ_{tot}^*	(b,c)
37	He	V	+23	1.5	DM, σ_{tot}^*	(b,c)
37	He	Cr	+24	1.5	DM, σ_{tot}^*	(b,c)
37	He	Mn	+25	1.5	DM, σ_{tot}^*	(b,c)
40	He	Xe	+03	5-3700	VPS-Emp	---
40	He	Xe	+04	3-4700	VPS-Emp	---
40	He	Xe	+06	2-5600	VPS-Emp	---
40	He	Xe	+08	1-7400	VPS-Emp	---
40	He	Xe	+10	1-9400	VPS-Emp	---
8	Li	He	+02	0.05-2	PSS (12 states)	(c)
18	Li	He	+02	0.1-20	CC-AO (40 states)	(a)
43	Li	He	+02	2-25	CC-AO (2 states)	(b)
8	Li	He	+02	7.5-47	CTMC, Z_{eff}	(b)
44	Li	He	+02	50-400	CTMC, Z_{eff}	(b)
37	Li	B	+05	1.32	DM, σ_{tot}^*	(b,c)
37	Li	C	+06	1.32	DM, σ_{tot}^*	(b,c)
37	Li	N	+07	1.32	DM, σ_{tot}^*	(b,c)
37	Li	O	+08	1.32	DM, σ_{tot}^*	(b,c)
37	Li	F	+09	1.32	DM, σ_{tot}^*	(b,c)
42	Li	Ne	+10	0.76	DM, σ_{tot}^*	(b,c)
37	Li	Ne	+10	1.32	DM, σ_{tot}^*	(b,c)
37	Li	Na	+11	1.32	DM, σ_{tot}^*	(b,c)
37	Li	Mg	+12	1.32	DM, σ_{tot}^*	(b,c)
37	Li	Aℓ	+13	1.32	DM, σ_{tot}^*	(b,c)
37	Li	Si	+14	1.32	DM, σ_{tot}^*	(b,c)
37	Li	P	+15	1.32	DM, σ_{tot}^*	(b,c)
37	Li	S	+16	1.32	DM, σ_{tot}^*	(b,c)
37	Li	Cℓ	+17	1.32	DM, σ_{tot}^*	(b,c)
37	Li	Ar	+18	1.32	DM, σ_{tot}^*	(b,c)

Table 1. Sources of theoretical data for charge transfer between atoms ($Z \leq 2$) and ions ($q \geq 2$) (cont'd.)

Reference	Target Atomic Species	Projectile Ionic Species	Ionic Charge State	Energy Range (keV/u)	Method and Comments[a]	Accuracy
37	Li	K	+19	1.32	DM, σ_{tot}*	(b,c)
37	Li	Ca	+20	1.32	DM, σ_{tot}*	(b,c)
37	Li	Sc	+21	1.32	DM, σ_{tot}*	(b,c)
37	Li	Sc	+21	1.32	DM, σ_{tot}*	(b,c)
37	Li	Ti	+22	1.32	DM, σ_{tot}*	(b,c)
37	Li	V	+23	1.32	DM, σ_{tot}*	(b,c)
37	Li	Cr	+24	1.32	DM, σ_{tot}*	(b,c)
37	Li	Mn	+25	1.32	DM, σ_{tot}*	(b,c)
37	Li	Fe	+26	1.32	DM, σ_{tot}*	(b,c)
37	Li	Ne	+10	1.32	DM, σ_{tot}*	(b,c)
37	Li	Co	+27	1.32	DM, σ_{tot}*	(b,c)
37	Li	Ni	+28	1.32	DM, σ_{tot}*	(b,c)
37	Li	Cu	+29	1.32	DM, σ_{tot}*	(b,c)
37	Li	Zn	+30	1.32	DM, σ_{tot}*	(b,c)
37	Li	Ga	+31	1.32	DM, σ_{tot}*	(b,c)
37	Li	Ge	+32	1.32	DM, σ_{tot}*	(b,c)
37	Li	As	+33	1.32	DM, σ_{tot}*	(b,c)
37	Li	Se	+34	1.32	DM, σ_{tot}*	(b,c)
37	Li	Br	+35	1.32	DM, σ_{tot}*	(b,c)
37	Li	Kr	+36	1.32	DM, σ_{tot}*	(b,c)
37	Li	Rb	+37	1.32	DM, σ_{tot}*	(b,c)
37	Li	Sr	+38	1.32	DM, σ_{tot}*	(b,c)
37	Li	Y	+39	1.32	DM, σ_{tot}*	(b,c)
37	Li	Zr	+40	1.32	DM, σ_{tot}*	(b,c)
34	C	He	+02	770-3100	BK-Eik, Z_{eff}	(b)
34	C	Li	+03	770-3100	BK-Eik, Z_{eff}	(b)
40	N	O	+03	6-9000	VPS-Emp, σ_{sum}†	---
40	N	O	+06	6-14000	VPS-Emp. σ_{sum}†	---
40	N	O	+08	6-20000	VPS-Emp, σ_{sum}†	---
15	Ne	He	+02	400-4000	CC-AO (48+1 states) unitarity not preserved σ_K§	(a,b)
15	Ne	Li	+03	400-4000	CC-AO (48+1 states) unitarity not preserved σ_K§	(a,b)
34	Ne	Li	+03	770-3100	BK-Eik, Z_{eff}	(b)
37	Ne	B	+05	1.5	DM, σ_{tot}*	(b,c)
37	Ne	C	+06	1.5	DM, σ_{tot}*	(b,c)
39	Ne	N	+02	0.7-16	RF; stat. average	(d)
37	Ne	N	+07	1.5	DM, σ_{tot}*	(b,c)
45	Ne	N	+07	1000-1400	CC-AO (2 states); σ_{K-K}	(b)
10	Ne	O	+02	0.2-14	LZ; RF; stat. average	(c)
37	Ne	O	+08	1.5	DM, σ_{tot}*	(b,c)
45	Ne	O	+08	1500-2200	CC-AO (2 states); σ_{K-K}	(b,c)
37	Ne	F	+09	1.5	DM, σ_{tot}*	(b,c)
45	Ne	F	+09	1000-1600	CC-AO (2 states). σ_{K-K}	(b,c)
42	Ne	Ne	+10	0.76	DM, σ_{tot}*	(b,c)
37	Ne	Ne	+10	1.5	DM, σ_{tot}*	(b,c)
37	Ne	Na	+11	1.5	DM, σ_{tot}*	(b,c)

Table 1. Sources of theoretical data for charge transfer between atoms ($Z \geq 2$) and ions ($q \geq 2$) (cont'd.)

Reference	Target Atomic Species	Projectile Ionic Species	Ionic Charge State	Energy Range (keV/amu)	Method and Comments[a]	Accuracy
37	Ne	Mg	+12	1.5	DM, σ_{tot}^{*}	(b,c)
37	Ne	Aℓ	+13	1.5	DM, σ_{tot}^{*}	(b,c)
37	Ne	Si	+14	1.5	DM, σ_{tot}^{*}	(b,c)
37	Ne	P	+15	1.5	DM, σ_{tot}^{*}	(b,c)
37	Ne	S	+16	1.5	DM, σ_{tot}^{*}	(b,c)
37	Ne	Cℓ	+17	1.5	DM, σ_{tot}^{*}	(b,c)
42	Ne	Ar	+03	0.75	DM, σ_{tot}^{*}	(c)
42	Ne	Ar	+04	0.75	DM, σ_{tot}^{*}	(c)
42	Ne	Ar	+05	0.75	DM, σ_{tot}^{*}	(c)
42	Ne	Ar	+06	0.75	DM, σ_{tot}^{*}	(c)
42	Ne	Ar	+07	0.75	DM, σ_{tot}^{*}	(c)
42	Ne	Ar	+08	0.75	DM, σ_{tot}^{*}	(c)
42	Ne	Ar	+09	0.75	DM, σ_{tot}^{*}	(c)
37	Ne	Ar	+18	1.5	DM, σ_{tot}^{*}	(b,c)
37	Ne	K	+19	1.5	DM, σ_{tot}^{*}	(b,c)
37	Ne	Ca	+20	1.5	DM, σ_{tot}^{*}	(b,c)
37	Ne	Sc	+21	1.5	DM, σ_{tot}^{*}	(b,c)
37	Ne	Ti	+22	1.5	DM, σ_{tot}^{*}	(b,c)
37	Ne	V	+23	1.5	DM, σ_{tot}^{*}	(b,c)
37	Ne	Cr	+24	1.5	DM, σ_{tot}^{*}	(b,c)
37	Ne	Mn	+25	1.5	DM, σ_{tot}^{*}	(b,c)
46	Ne	Kr	+03	0.005-1.4	M-VPS	(b)
40	Ne	Xe	+02	2-9000	VPS-Emp, $\sigma_{sum}^{\dagger}$	---
40	Ne	Xe	+04	2-13500	VPS-Emp, $\sigma_{sum}^{\dagger}$	---
40	Ne	Xe	+08	1-23400	VPS-Emp, $\sigma_{sum}^{\dagger}$	---
40	Ne	Xe	+10	1-35000	VPS-Emp, $\sigma_{sum}^{\dagger}$	---
37	Na	B	+05	1.32	DM, σ_{tot}^{*}	(b,c)
37	Na	C	+06	1.32	DM, σ_{tot}^{*}	(b,c)
37	Na	N	+07	1.32	DM, σ_{tot}^{*}	(b,c)
37	Na	O	+08	1.32	DM, σ_{tot}^{*}	(b,c)
37	Na	F	+09	1.32	DM, σ_{tot}^{*}	(b,c)
37	Na	Ne	+10	1.32	DM, σ_{tot}^{*}	(b,c)
37	Na	Na	+11	1.32	DM, σ_{tot}^{*}	(b,c)
37	Na	Mg	+12	1.32	DM, σ_{tot}^{*}	(b,c)
37	Na	Aℓ	+13	1.32	DM, σ_{tot}^{*}	(b,c)
37	Na	Si	+14	1.32	DM, σ_{tot}^{*}	(b,c)
37	Na	P	+15	1.32	DM, σ_{tot}^{*}	(b,c)
37	Na	S	+16	1.32	DM, σ_{tot}^{*}	(b,c)
37	Na	Cℓ	+17	1.32	DM, σ_{tot}^{*}	(b,c)
37	Na	Ar	+18	1.32	DM, σ_{tot}^{*}	(b,c)
37	Na	K	+19	1.32	DM, σ_{tot}^{*}	(b,c)
37	Na	Ca	+20	1.32	DM, σ_{tot}^{*}	(b,c)
37	Na	Ti	+22	1.32	DM, σ_{tot}^{*}	(b,c)
37	Na	V	+23	1.32	DM, σ_{tot}^{*}	(b,c)
37	Na	Cr	+24	1.32	DM, σ_{tot}^{*}	(b,c)
37	Na	Mn	+25	1.32	DM, σ_{tot}^{*}	(b,c)
37	Na	Fe	+26	1.32	DM, σ_{tot}^{*}	(b,c)
37	Na	Co	+27	1.32	DM, σ_{tot}^{*}	(b,c)

Table 1. Sources of theoretical data for charge transfer between atoms ($Z \leq 2$) and ions ($q \leq 2$) (cont'd.)

Reference	Target Atomic Species	Projectile Ionic Species	Ionic Charge State	Energy Range (keV/u)	Method and Comments[a]	Accuracy
37	Na	Ni	+28	1.32	DM, σ_{tot}^{*}	(b,c)
37	Na	Cu	+29	1.32	DM, σ_{tot}^{*}	(b,c)
37	Na	Zn	+30	1.32	DM, σ_{tot}^{*}	(b,c)
37	Na	Ga	+31	1.32	DM, σ_{tot}^{*}	(b,c)
37	Na	Ge	+32	1.32	DM, σ_{tot}^{*}	(b,c)
37	Na	As	+33	1.32	DM, σ_{tot}^{*}	(b,c)
37	Na	Se	+34	1.32	DM, σ_{tot}^{*}	(b,c)
37	Na	Br	+35	1.32	DM, σ_{tot}^{*}	(b,c)
37	Na	Kr	+36	1.32	DM, σ_{tot}^{*}	(b,c)
37	Na	Rb	+37	1.32	DM, σ_{tot}^{*}	(b,c)
37	Na	Sr	+38	1.32	DM, σ_{tot}^{*}	(b,c)
37	Na	Y	+39	1.32	DM, σ_{tot}^{*}	(b,c)
37	Na	Zr	+40	1.32	DM, σ_{tot}^{*}	(b,c)
47	Si	F	+09	400-2400	PSS (2 states), σ_{K-K}	(b,c)
48	Si	F	+09	70-770	CC-MO (2 states) Variable screening model	(c,d)
49	Si	F	+09	400-2200	CC-AO (2 states) Herman-Skillman potential σ_{K-K}	(b,c)
21	Si	Si	+14	100-90000	N-BK	---
16	Ar	He	+02	1000-9000	CC-AO (+ pseudostates), σ_K[§] Unitarity not preserved	(a,b)
37	Ar	B	+05	1.5	DM, σ_{tot}^{*}	(b,c)
16	Ar	C	+04	1000-8000	CC-AO (+ pseudostates), σ_K[§]	(a,b)
37	Ar	C	+06	1.5	DM, σ_{tot}^{*}	(b,c)
16	Ar	C	+06	1000-9000	CC-AO (+ pseudostates), σ_K[§]	(a,b)
45	Ar	C	+06	1000-2000	CC-AO (2 states), σ_{K-K}	(a,b)
39	Ar	N	+02	0.7-16	RF, stat. average	(d)
37	Ar	N	+07	1.5	DM, σ_{tot}^{*}	(b,c)
45	Ar	N	+07	1000-2000	CC-AO (2 states), σ_{K-K}	(b,c)
10	Ar	O	+02	0.2-14	LZ; RF, stat. average	(c)
37	Ar	O	+08	1.5	DM, σ_{tot}^{*}	(b,c)
40	Ar	F	+07	6-56000	VPS-Emp, $\sigma_{sum}^{\dagger}$	---
37	Ar	F	+09	1.5	DM, σ_{tot}^{*}	(b,c)
49	Ar	F	+09	1000-4000	CC-AO (2 states; Herman-Skillman screening σ_{K-K}	(b,c)
45	Ar	F	+09	1000-4000	CC-AO (2 states), σ_{K-K}	(b)
42	Ar	Ne	+10	0.76	DM, σ_{tot}^{*}	(b,c)
37	Ar	Ne	+10	1.5	DM, σ_{tot}^{*}	(b,c)
37	Ar	Na	+11	1.5	DM, σ_{tot}^{*}	(b,c)
37	Ar	Mg	+12	1.5	DM, σ_{tot}^{*}	(b,c)
37	Ar	Al	+13	1.5	DM, σ_{tot}^{*}	(b,c)
37	Ar	Si	+14	1.5	DM, σ_{tot}^{*}	(b,c)
37	Ar	P	+15	1.5	DM, σ_{tot}^{*}	(b,c)
37	Ar	S	+16	1.5	DM, σ_{tot}^{*}	(b,c)
37	Ar	Cl	+17	1.5	DM, σ_{tot}^{*}	(b,c)
50	Ar	Ar	+04	1.1		
50	Ar	Ar	+05	1.1		
42	Ar	Ar	+06	0.05-3.4	DM, σ_{tot}^{*}	(b)

Table 1. Sources of theoretical data for charge transfer between atoms ($Z \leq 2$) and ions ($q \leq 2$) (cont'd.)

Reference	Target Atomic Species	Projectile Ionic Species	Ionic Charge State	Energy Range (keV/u)	Method and Comments[a]	Accuracy
50	Ar	Ar	+06	1.1		
42	Ar	Ar	+07	0.06-3.3	DM, σ_{tot}^*	(b,c)
50	Ar	Ar	+07	1.1		
37	Ar	Ar	+18	1.5	DM, σ_{tot}^*	(b,c)
37	Ar	K	+19	1.5	DM, σ_{tot}^*	(b,c)
37	Ar	Ca	+20	1.5	DM, σ_{tot}^*	(b,c)
37	Ar	Sc	+21	1.5	DM, σ_{tot}^*	(b,c)
37	Ar	Ti	+22	1.5	DM, σ_{tot}^*	(b,c)
37	Ar	V	+23	1.5	DM, σ_{tot}^*	(b,c)
37	Ar	Cr	+24	1.5	DM, σ_{tot}^*	(b,c)
37	Ar	Mn	+25	1.5	DM, σ_{tot}^*	(b,c)
37	K	B	+05	1.32	DM, σ_{tot}^*	(b,c)
37	K	C	+06	1.32	DM, σ_{tot}^*	(b,c)
37	K	N	+07	1.32	DM, σ_{tot}^*	(b,c)
37	K	O	+08	1.32	DM, σ_{tot}^*	(b,c)
37	K	F	+09	1.32	DM, σ_{tot}^*	(b,c)
42	K	Ne	+10	0.76	DM, σ_{tot}^*	(b,c)
37	K	Ne	+10	1.32	DM, σ_{tot}^*	(b,c)
37	K	Na	+11	1.32	DM, σ_{tot}^*	(b,c)
37	K	Mg	+12	1.32	DM, σ_{tot}^*	(b,c)
37	K	Al	+13	1.32	DM, σ_{tot}^*	(b,c)
37	K	Si	+14	1.32	DM, σ_{tot}^*	(b,c)
37	K	P	+15	1.32	DM, σ_{tot}^*	(b,c)
37	K	S	+16	1.32	DM, σ_{tot}^*	(b,c)
37	K	Cl	+17	1.32	DM, σ_{tot}^*	(b,c)
37	K	Ar	+18	1.32	DM, σ_{tot}^*	(b,c)
37	K	K	+19	1.32	DM, σ_{tot}^*	(b,c)
37	K	Ca	+20	1.32	DM, σ_{tot}^*	(b,c)
37	K	Sc	+21	1.32	DM, σ_{tot}^*	(b,c)
37	K	Ti	+22	1.32	DM, σ_{tot}^*	(b,c)
37	K	V	+23	1.32	DM, σ_{tot}^*	(b,c)
37	K	Cr	+24	1.32	DM, σ_{tot}^*	(b,c)
37	K	Mn	+25	1.32	DM, σ_{tot}^*	(b,c)
37	K	Fe	+26	1.32	DM, σ_{tot}^*	(b,c)
37	K	Co	+27	1.32	DM, σ_{tot}^*	(b,c)
37	K	Ni	+28	1.32	DM, σ_{tot}^*	(b,c)
37	K	Cu	+29	1.32	DM, σ_{tot}^*	(b,c)
37	K	Zn	+30	1.32	DM, σ_{tot}^*	(b,c)
37	K	Ga	+31	1.32	DM, σ_{tot}^*	(b,c)
37	K	Ge	+32	1.32	DM, σ_{tot}^*	(b,c)
37	K	As	+33	1.32	DM, σ_{tot}^*	(b,c)
37	K	Se	+34	1.32	DM, σ_{tot}^*	(b,c)
37	K	Br	+35	1.32	DM, σ_{tot}^*	(b,c)
37	K	Kr	+36	1.32	DM, σ_{tot}^*	(b,c)
37	K	Rb	+37	1.32	DM, σ_{tot}^*	(b,c)
37	K	Sr	+38	1.32	DM, σ_{tot}^*	(b,c)
37	K	Y	+39	1.32	DM, σ_{tot}^*	(b,c)

Table 1. Sources of theoretical data for charge transfer between atoms ($Z \leq 2$) and ions ($q \leq 2$) (cont'd.)

Reference	Target Atomic Species	Projectile Ionic Species	Ionic Charge State	Energy Range (keV/u)	Method and Comments[a]	Accuracy
37	K	Zr	+40	1.32	DM, σ_{tot}^{*}	(b,c)
19	Sc	Si	+14	1930	CC-AO (2 states), σ_{K-K}	(c)
16	Ti	He	+02	2000-8000	CC-AO (+ pseudostates)	(a,b)
19	Ti	Si	+14	1930	CC-AO (2 states), σ_{K-K}	(c)
17	Cu	He	+02	6070	CC-AO (+ pseudostates) 27+1 states $\sigma_K^{\S}$, $\sigma_L^{\S}$	(a,b)
17	Cu	C	+06	6070	CC-AO (+ pseudostates) 27+1 states $\sigma_K^{\S}$, $\sigma_L^{\S}$	(a,b)
17	Cu	O	+08	6070	CC-AO (+ pseudostates) 27+1 states $\sigma_K^{\S}$, $\sigma_L^{\S}$	(a,b)
19	Cu	Si	+14	1930	CC-AO (2 states), σ_{K-K}	(d)
19	Cu	S	+16	1710	CC-AO (2 states), σ_{K-K}	(b)
19	Cu	Cℓ	+17	1710	CC-AO (2 states), σ_{K-K}	(b)
37	Kr	B	+05	1.5	DM, σ_{tot}^{*}	(b,c)
37	Kr	C	+06	1.5	DM, σ_{tot}^{*}	(b,c)
37	Kr	N	+07	1.5	DM, σ_{tot}^{*}	(b,c)
39	Kr	N	+02	3-15	RF, stat. average	(d)
10	Kr	O	+02	0.3-14	LZ; RF stat. average	(c)
37	Kr	O	+08	1.5	DM, σ_{tot}^{*}	(b,c)
37	Kr	F	+09	1.5	DM, σ_{tot}^{*}	(b,c)
45	Kr	F	+09	2400-4000	CC-AO (2 states), σ_{K-K}	(b,c)
42	Kr	Ne	+10	0.76	DM, σ_{tot}^{*}	(b,c)
37	Kr	Ne	+10	1.5	DM, σ_{tot}^{*}	(b,c)
37	Kr	Na	+11	1.5	DM, σ_{tot}^{*}	(b,c)
37	Kr	Mg	+12	1.5	DM, σ_{tot}^{*}	(b,c)
37	Kr	Aℓ	+13	1.5	DM, σ_{tot}^{*}	(b,c)
37	Kr	Si	+14	1.5	DM, σ_{tot}^{*}	(b,c)
37	Kr	P	+15	1.5	DM, σ_{tot}^{*}	(b,c)
37	Kr	S	+16	1.5	DM, σ_{tot}^{*}	(b,c)
45	Kr	Cℓ	+17	2800-4500	CC-AO (2 states), σ_{K-K}	(b,c)
37	Kr	Cℓ	+17	1.5	DM, σ_{tot}^{*}	(b,c)
37	Kr	Ar	+18	1.5	DM, σ_{tot}^{*}	(b,c)
37	Kr	K	+19	1.5	DM, σ_{tot}^{*}	(b,c)
37	Kr	Ca	+20	1.5	DM, σ_{tot}^{*}	(b,c)
37	Kr	Sc	+21	1.5	DM, σ_{tot}^{*}	(b,c)
37	Kr	Ti	+22	1.5	DM, σ_{tot}^{*}	(b,c)
37	Kr	V	+23	1.5	DM, σ_{tot}^{*}	(b,c)
37	Kr	Cr	+24	1.5	DM, σ_{tot}^{*}	(b,c)
37	Kr	Mn	+25	1.5	DM, σ_{tot}^{*}	(b,c)
42	Kr	Xe	+03	0.23	DM, σ_{tot}^{*}	(b,c)
42	Kr	Xe	+04	0.23	DM, σ_{tot}^{*}	(b,c)
42	Kr	Xe	+05	0.23	DM, σ_{tot}^{*}	(b,c)
42	Kr	Xe	+06	0.23	DM, σ_{tot}^{*}	(b,c)
42	Kr	Xe	+07	0.23	DM, σ_{tot}^{*}	(b,c)
42	Kr	Xe	+08	0.23	DM, σ_{tot}^{*}	(b,c)
42	Kr	Xe	+09	0.23	DM, σ_{tot}^{*}	(b,c)

Table 1. Sources of theoretical data for charge transfer between atoms ($Z \leq 2$) and ions ($q \leq 2$) (cont'd.)

Reference	Target Atomic Species	Projectile Ionic Species	Ionic Charge State	Energy Range (keV/u)	Method and Comments[a]	Accuracy
37	Rb	B	+05	1.32	DM, σ_{tot}^*	(b,c)
37	Rb	C	+06	1.32	DM, σ_{tot}^*	(b,c)
37	Rb	N	+07	1.32	DM, σ_{tot}^*	(b,c)
37	Rb	O	+08	1.32	DM, σ_{tot}^*	(b,c)
37	Rb	F	+09	1.32	DM, σ_{tot}^*	(b,c)
37	Rb	Ne	+10	1.32	DM, σ_{tot}^*	(b,c)
37	Rb	Na	+11	1.32	DM, σ_{tot}^*	(b,c)
37	Rb	Mg	+12	1.32	DM, σ_{tot}^*	(b,c)
37	Rb	Aℓ	+13	1.32	DM, σ_{tot}^*	(b,c)
37	Rb	Si	+14	1.32	DM, σ_{tot}^*	(b,c)
37	Rb	P	+15	1.32	DM, σ_{tot}^*	(b,c)
37	Rb	S	+16	1.32	DM, σ_{tot}^*	(b,c)
37	Rb	Cℓ	+17	1.32	DM, σ_{tot}^*	(b,c)
37	Rb	Ar	+18	1.32	DM, σ_{tot}^*	(b,c)
37	Rb	K	+19	1.32	DM, σ_{tot}^*	(b,c)
37	Rb	Ca	+20	1.32	DM, σ_{tot}^*	(b,c)
37	Rb	Sc	+21	1.32	DM, σ_{tot}^*	(b,c)
37	Rb	Ti	+22	1.32	DM, σ_{tot}^*	(b,c)
37	Rb	V	+23	1.32	DM, σ_{tot}^*	(b,c)
37	Rb	Cr	+24	1.32	DM, σ_{tot}^*	(b,c)
37	Rb	Mn	+25	1.32	DM, σ_{tot}^*	(b,c)
37	Rb	Fe	+26	1.32	DM, σ_{tot}^*	(b,c)
37	Rb	Co	+27	1.32	DM, σ_{tot}^*	(b,c)
37	Rb	Ni	+28	1.32	DM, σ_{tot}^*	(b,c)
37	Rb	Cu	+29	1.32	DM, σ_{tot}^*	(b,c)
37	Rb	Zn	+30	1.32	DM, σ_{tot}^*	(b,c)
37	Rb	Ga	+31	1.32	DM, σ_{tot}^*	(b,c)
37	Rb	Ge	+32	1.32	DM, σ_{tot}^*	(b,c)
37	Rb	As	+33	1.32	DM, σ_{tot}^*	(b,c)
37	Rb	Se	+34	1.32	DM, σ_{tot}^*	(b,c)
37	Rb	Br	+35	1.32	DM, σ_{tot}^*	(b,c)
37	Rb	Kr	+36	1.32	DM, σ_{tot}^*	(b,c)
37	Rb	Rb	+37	1.32	DM, σ_{tot}^*	(b,c)
37	Rb	Sr	+38	1.32	DM, σ_{tot}^*	(b,c)
37	Rb	Y	+39	1.32	DM, σ_{tot}^*	(b,c)
37	Rb	Zr	+40	1.32	DM, σ_{tot}^*	(b,c)
37	Xe	B	+05	1.5	DM, σ_{tot}^*	(b,c)
37	Xe	C	+06	1.5	DM, σ_{tot}^*	(b,c)
39	Xe	N	+02	2-15	RF, stat. average	(d)
37	Xe	N	+07	1.5	DM, σ_{tot}^*	(b,c)
10	Xe	O	+02	0.3-14	LZ; RF; stat. average	(c)
37	Xe	O	+08	1.5	DM, σ_{tot}^*	(b,c)
37	Xe	F	+09	1.5	DM, σ_{tot}^*	(b,c)
42	Xe	Ne	+10	0.76	DM, σ_{tot}^*	(b,c)
37	Xe	Ne	+10	1.5	DM, σ_{tot}^*	(b,c)
37	Xe	Na	+11	1.5	DM, σ_{tot}^*	(b,c)
37	Xe	Mg	+12	1.5	DM, σ_{tot}^*	(b,c)
37	Xe	Aℓ	+13	1.5	DM, σ_{tot}^*	(b,c)

Table 1. Sources of theoretical data for charge transfer between atoms ($Z \leq 2$) and ions ($q \leq 2$) (cont'd.)

Reference	Target Atomic Species	Projectile Ionic Species	Ionic Charge State	Energy Range (keV/u)	Method and Comments[a]	Accuracy
37	Xe	Si	+14	1.5	DM, σ_{tot}^*	(b,c)
37	Xe	P	+15	1.5	DM, σ_{tot}^*	(b,c)
37	Xe	S	+16	1.5	DM, σ_{tot}^*	(b,c)
37	Xe	Cℓ	+17	1.5	DM, σ_{tot}^*	(b,c)
42	Xe	Ar	+03	0.75	DM, σ_{tot}^*	(b,c)
42	Xe	Ar	+04	0.75	DM, σ_{tot}^*	(b,c)
42	Xe	Ar	+05	0.75	DM, σ_{tot}^*	(b,c)
42	Xe	Ar	+06	0.75	DM, σ_{tot}^*	(b,c)
42	Xe	Ar	+07	0.75	DM, σ_{tot}^*	(b,c)
42	Xe	Ar	+08	0.75	DM, σ_{tot}^*	(b,c)
42	Xe	Ar	+09	0.75	DM, σ_{tot}^*	(b,c)
37	Xe	Ar	+18	1.5	DM, σ_{tot}^*	(b,c)
37	Cs	B	+05	1.32	DM, σ_{tot}^*	(b,c)
37	Cs	C	+06	1.32	DM, σ_{tot}^*	(b,c)
37	Cs	C	+06	1.32	DM, σ_{tot}^*	(b,c)
37	Cs	N	+07	1.32	DM, σ_{tot}^*	(b,c)
37	Cs	O	+08	1.32	DM, σ_{tot}^*	(b,c)
37	Cs	F	+09	1.32	DM, σ_{tot}^*	(b,c)
42	Cs	Ne	+10	0.75	DM, σ_{tot}^*	(b,c)
37	Cs	Ne	+10	1.32	DM, σ_{tot}^*	(b,c)
37	Cs	Na	+11	1.32	DM, σ_{tot}^*	(b,c)
37	Cs	Mg	+12	1.32	DM, σ_{tot}^*	(b,c)
37	Cs	Aℓ	+13	1.32	DM, σ_{tot}^*	(b,c)
37	Cs	Si	+14	1.32	DM, σ_{tot}^*	(b,c)
37	Cs	P	+15	1.32	DM, σ_{tot}^*	(b,c)
37	Cs	S	+16	1.32	DM, σ_{tot}^*	(b,c)
37	Cs	Cℓ	+17	1.32	DM, σ_{tot}^*	(b,c)
37	Cs	Ar	+18	1.32	DM, σ_{tot}^*	(b,c)
37	Cs	K	+19	1.32	DM, σ_{tot}^*	(b,c)
37	Cs	Ca	+20	1.32	DM, σ_{tot}^*	(b,c)
37	Cs	Sc	+21	1.32	DM, σ_{tot}^*	(b,c)
37	Cs	Ti	+22	1.32	DM, σ_{tot}^*	(b,c)
37	Cs	V	+23	1.32	DM, σ_{tot}^*	(b,c)
37	Cs	Cr	+24	1.32	DM, σ_{tot}^*	(b,c)
37	Cs	Mn	+25	1.32	DM, σ_{tot}^*	(b,c)
37	Cs	Fe	+26	1.32	DM, σ_{tot}^*	(b,c)
37	Cs	Co	+27	1.32	DM, σ_{tot}^*	(b,c)
37	Cs	Ni	+28	1.32	DM, σ_{tot}^*	(b,c)
37	Cs	Cu	+29	1.32	DM, σ_{tot}^*	(b,c)
37	Cs	Zn	+30	1.32	DM, σ_{tot}^*	(b,c)
37	Cs	Ga	+31	1.32	DM, σ_{tot}^*	(b,c)
37	Cs	Ge	+32	1.32	DM, σ_{tot}^*	(b,c)
37	Cs	As	+33	1.32	DM, σ_{tot}^*	(b,c)
37	Cs	Se	+34	1.32	DM, σ_{tot}^*	(b,c)
37	Cs	Kr	+36	1.32	DM, σ_{tot}^*	(b,c)

[a]Abbreviations used in Table 1:

CC-MO	- molecular-orbital close-coupling method
PSS	- perturbed stationary state method
DM	- decay model (electron tunneling theory)
ASM	- absorbing sphere model
LZ	- Landau-Zener model (2 states)
RF	- Rapp-Fransis formula (2 states)
AM	- asymptotic method (2 states)
AM-Res	- asymptotic method for resonant processes (2 states)
RZD	- Rosen-Zener-Demkov model (2 states)
CC-AO	- atomic-orbital close-coupling method
UDWA	- unitarized distorted wave approximation
CTMC	- classical trajectory Monte Carlo method
VPS-Emp	- Vainshtein-Presnyakov-Sobelman approximation, with empirical normalization
M-VPS	- Multichannel VPS approximation
BK	- Brinkmann-Kramers approximation
BK-Emp	- BK with empirical normalization factor (of 0.138)
NBK	- non-empirically normalized BK
B1	- first Born approximation
B-B1	- Bates-Born approximation
CPB	- Coulomb projected Born approximation
BK-Eik	- eikonal Brinkmann-Kramers approximation
CDW	- continuum distorted wave method

*σ_{tot} contains the contribution of one-, two- and more-electron capture.

†Contribution to σ_{sum} from inner-shell electrons included.

§Total cross section for K- (or L-) vacancy production by charge transfer.

#Reaction rate constant.

Table 2. Sources of theoretical data for charge exchange cross sections in ion-ion collisions

Reference	Projectile	Target	Energy Range keV/u	Method	Comment	Accuracy
			a. Single charge exchange			
25	He^{2+}	He^{+}	0.005-25	AM-Res	Correct exchange coupling	(b,c)
25	Li^{3+}	Li^{2+}	0.015-25	AM-Res	"	(b,c)
25	Be^{4+}	Be^{3+}	0.025-25	AM-Res	"	(b,c)
25	B^{5+}	B^{4+}	0.04-25	AM-Res	"	(b,c)
25	C^{6+}	C^{5+}	0.09-25	AM-Res	"	(b,c)
25	N^{7+}	N^{6+}	0.12-25	AM-Res	"	(b,c)
25	O^{8+}	O^{7+}	0.18-25	AM-Res	"	(b,c)
27	He^{2+}	O^{2+}	0.031-31	RZD		
27	C^{2+}	B^{+}	0.018-18	RZD		(b,c)
27	N^{3+}	C^{2+}	0.016-16	RZD		(b,c)
27	O^{4+}	N^{3+}	0.013-13	RZD		(b,c)
27	F^{5+}	O^{4+}	0.012-12	RZD		(b,c)
27	Ne^{6+}	F^{5+}	0.010-10	RZD		(b,c)
51	O^{+}	C^{6+}	0.15, 0.73	LZ	Coulomb trajectory effects neglected	(c,d)
51	C^{+}	N^{7+}	0.16, 0.77	LZ	"	(c,d)
51	C^{3+}	N^{7+}	0.16, 0.77	LZ	"	(c,d)
51	N^{+}	N^{7+}	0.14, 0.71	LZ	"	(c,d)
51	O^{2+}	N^{7+}	0.13, 0.67	LZ	"	(c,d)
51	N^{3+}	O^{8+}	0.13, 0.67	LZ	"	(c,d)
51	O^{+}	O^{8+}	0.13, 0.63	LZ	"	(c,d)
51	O^{3+}	O^{8+}	0.13, 0.63	LZ	"	(c,d)
52	He^{2+}	He^{+}	100-300	CTMC	"	(b)
53	He^{2+}	O^{3+}	250-500	CTMC	Z_{eff}	(b,c)
53	He^{2+}	O^{4+}	250-500	CTMC	Z_{eff}	(b,c)
53	He^{2+}	O^{5+}	250-500	CTMC	Z_{eff}	(b,c)
29	He^{2+}	He^{+}	100, 500	CDW	$\sigma_{1s,1s}$; $\sigma_{1s,2s}$	(a,b)
29	He^{2+}	Li^{2+}	100, 500	CDW	$\sigma_{1s,1s}$; $\sigma_{1s,2s}$	(a,b)
29	He^{2+}	Be^{3+}	100, 500	CDW	$\sigma_{1s,1s}$; $\sigma_{1s,2s}$	(a,b)
24	He^{2+}	Li^{+}	25-750	CDW	σ_{+} (n^{-3} rule) 35-term, CI w.f.	(a,b), $E \geq 100$ (c), $E < 100$
54	He^{2+}	He^{+}	25, 5000	CPB		(c,d)
54	He^{2+}	Li^{2+}	50, 5000	CPB		(c,d)
54	He^{2+}	B^{3+}	50, 5000	CPB		(c,d)
54	He^{2+}	C^{5+}	125, 50,000	CPB		(c,d)
54	He^{2+}	Fe^{25+}	2500, 125,000	CPB		(c,d)
28	Ba^{+}	Ba^{+}	0.18-3.64	CC-MO	six $^1\Sigma$ and six $^3\Sigma$ states; σ_t - stat. average	(a,b)
			b. Double electron capture			
26	Li^{3+}	Li^{+}	0.0086-43	AM-Res	correct exchange coupling	(b,c)
26	Be^{4+}	Be^{2+}	0.0222-22	AM-Res	"	(b,c)
26	B^{5+}	B^{3+}	0.046-28	AM-Res	"	(b,c)
26	C^{6+}	C^{4+}	0.075-25	AM-Res	"	(b,c)
26	N^{7+}	N^{5+}	14-57	AM-Res	"	(b,c)
26	O^{8+}	O^{6+}	19-53	AM-Res	"	(b,c)
26	F^{9+}	F^{7+}	21-42	AM-Res	"	(b,c)
26	Ne^{10+}	Ne^{8+}	25-40	AM-Res	"	(b,c)
26	B^{3+}	B^{+}	0.0026-28	AM-Res	"	(b,c)
26	C^{4+}	C^{2+}	0.0079-25	AM-Res	"	(b,c)
26	N^{4+}	N^{2+}	0.014-21	AM-Res	"	(b,c)
26	O^{6+}	O^{4+}	0.022-20	AM-Res	"	(b,c)

Table 3. Sources of theoretical data for double charge exchange cross sections in ion-atom collisions

Reference	Projectile	Target	Energy Range keV/u	Method	Comment	Accuracy
55	$^4He^{2+}$	He	0.05-2.5	CC-MO	2-states; correct molecular energies	(b)
56	$^3He^{2+}$	He	0.5-6.67	AM-Res	2-states	(b)
30	$^3He^{2+}$	He	0.5-12	AM-Res	2-states	(b)
5	$^3He^{2+}$	He	3.33-33.3	PSS	16-states	(a,b)
57	He^{2+}	He	25-250	CC-AO	3-states, σ_K[§]	(b,c)
59	He^{2+}	He	---	CC-AO	3-states, σ_{diff}	---
29	He^{2+}	He	1.25-375	CC-AO + perturbation method	9-states; 3 strongly coupled	(b,c) (b,c) (b,c)
33	He^{2+}	He	25-250	B-Bl	Independent electron model	---
58	He^{2+}	He	125-350	CDW, for single capture	"	(b,c)
30	C^{4+}	He	0.003-2.5	LZ	Correct (AM) splitting	(b)
6	C^{4+}	He	0.07-1.7	PSS	4-states	(b)
59	Ar^{6+}	He	0.05-2.5	classical		---
57	N^{7+}	Ne	700-4000	CC-AO	3-states, σ_K[§]	(c)
57	O^{8+}	Ne	900-2900	CC-AO	"	(c)
57	F^{9+}	Ne	1000-2000	CC-AO	"	(c)
58	F^{9+}	Ar	1580-3260	CDW, for single capture	σ_K[§], σ_L[§]	(b,c)

[§]See footnote to table 1.

Table 4. Validity regions and accuracy of different theoretical methods for charge exchange

Method	Velocity Range (v_e)	Comments	Accuracy
		A. Low-energy methods	
1) PSS/(CC-MO)	0.01-0.5	- numerical solution of coupled equations - classical (quantum) of nuclear motion, - translational factors optional	depends on the size of the basis
	0.5-1	- numerical solution of coupled equations - classical nuclear motion, - translational factors necessary,	depends on the size of the basis and the form of translational factors
2) LZ, RF, RZD, AM, AM-Res	0.02-0.6	- two-state models with radial coupling only	(b) or (c), if coupling with other channels small; otherwise (d)
3) ASM	0.2-0.6	- σ includes single- and more-electron captures, - no rotational coupling	(b) or (c), smaller v, high Z; (d), higher v, low z
4) DM	0.2-0.6	same	same
		B. Intermediate-energy methods	
1) CC-AO	0.2- ~3-4	- numerical solution of coupled equations - plane wave or Coulomb translational factors necessary	depends on number of basis states
2)	0.3- ~3-4	- unitarity preserved	(b), (c), $v \lesssim 2$ (d), $v > 2$
3) UDWA	0.7- ~3-4	- unitarity preserved	same
4) CTMC	1- ~3-4		(a) or (b), $v < 3$ (b) or (c), $v > 3$
5) VPS-Emp	0.3-3-4		unspecified
		C. High-energy methods	
1) BK	>2	- nucleus-nucleus interaction excluded - incorrect v-asymptotics	(d)
2) Bl, B-Bl, CPB	>2	-all interactions included - incorrect v-asymptotics	unspecified
3) BK-Eik	2-7		(b), (c)
4) CDW	≳4		(a), (b)
5) BK-Emp, N-BK	>2		unspecified

Table 5. Theoretical cross sections as functions of E/M (keV/u) for charge transfer in collisions of non-hydrogenic atoms with ions ($q > 2$). In this table, σ refers to single-electron capture from the outer shell; σ_{tot} contains the contribution of one-, two-, and more electron capture; σ_{sum} includes contributions from inner-shell electrons; and σ_K (and σ_L) is the total cross section for K- (or L-) vacancy production by charge transfer

He-He^{2+}

E/M	$\sigma(10^{-16}cm^2)$
2.18	0.356
3.95	0.444
5.09	0.465
6.25	0.509
7.55	0.693
8.93	0.780
12.2	1.04
15.9	1.54
20.2	1.97
25.1	2.19
33.4	2.30

Ref. 5

E/M	$\sigma(10^{-16}cm^2)$
38.7	2.38
51.1	2.36
88.6	1.35
111.	0.966
125.	0.332
160.	0.569
209.	0.323
265.	0.173
324.	0.088
359.	0.060
375.	0.051

Ref. 29

He-He^{2+}

E/M	$\sigma(10^{-16}cm^2)$
98.5	2.11
110.	1.14
122.	0.74
135.	0.54
149.	0.42

Ref. 31

E/M	$\sigma(10^{-16}cm^2)$
474.	0.0103
551.	0.0058
702.	0.0022
848.	0.0008

Ref. 32

E/M	$\sigma(10^{-16}cm^2)$
454.	0.447
838.	0.003

Ref. 34

E/M	$\sigma_{tot}(10^{-16}cm^2)$
125.	1.33
250.	0.146
500.	0.0106
1000.	0.0005

Ref. 24

He-He^{2+}

E/M	$\sigma(10^{-16}cm^2)$
148.	0.859
310.	0.074
657.	0.0034

Ref. 23

He-Li^{3+}

E/M	$\sigma(10^{-16}cm^2)$
10.0	11.2
16.6	10.1
24.7	8.87
41.4	6.73
62.0	4.66
92.5	2.92
128.	1.76
165.	1.14
209.	0.684
273.	0.401
355.	0.190
470.	0.070
603.	0.030
811.	0.011

Ref. 35

E/M	$\sigma(10^{-16}cm^2)$
124.	2.42
175.	1.25
203.	0.728

Ref. 31

He-Be^{3+}

E/M	$\sigma(10^{-16}cm^2)$
0.033	4.65
0.048	5.16
0.077	6.08
0.125	7.36
0.225	9.10
0.393	11.0
0.677	12.8
1.09	14.0
1.41	14.3
1.76	14.4
1.99	14.3
2.46	14.0
3.55	13.1
5.05	12.2

Ref. 6

He-Be^{4+}

E/M	$\sigma(10^{-16}cm^2)$
97.3	8.17
122.	4.53
150.	2.54
170.	2.72
198.	0.76

Ref. 31

Table 5. Theoretical charge transfer cross sections for nonhydrogenic atoms and ions ($q > 2$), (continued)

He–B^{3+}

E/M	$\sigma(10^{-16}cm^2)$
0.033	2.84
0.053	4.26
0.108	6.55
0.317	10.2
0.956	13.6

Ref. 7

He–B^{5+}

E/M	$\sigma_{tot}(10^{-16}cm^2)$
1.53	26.2

Ref. 37

E/M	$\sigma(10^{-16}cm^2)$
99.6	9.84
125.	7.05
147.	5.21
173.	3.14
198.	1.59
249.	1.33

Ref. 31

E/M	$\sigma(10^{-16}cm^2)$
321.	0.670
610.	0.062
917.	0.010
1320.	0.002

Ref. 20

He–C^{4+}

E/M	$\sigma(10^{-16}cm^2)$
0.200	0.042
0.289	0.077
0.445	0.142
0.734	0.287
1.09	0.470
1.47	0.634
2.07	0.842
2.92	1.11
3.91	1.37
5.23	1.67

Ref. 6

He–C^{6+}

E/M	$\sigma_{tot}(10^{-16}cm^2)$
1.53	30.4

Ref. 37

E/M	$\sigma(10^{-16}cm^2)$
100.	12.8
126.	10.6
150.	8.45
175.	3.95
200.	1.92
225.	2.86
250.	0.946

Ref. 31

E/M	$\sigma(10^{-16}cm^2)$
277.	2.65
401.	0.555
640.	0.072
1056.	0.008

Ref. 20

He–N^{7+}

E/M	$\sigma_{tot}(10^{-16}cm^2)$
1.53	38.7

Ref. 37

E/M	$\sigma(10^{-16}cm^2)$
98.7	17.0
125.	14.2
148.	11.8
173.	5.84
198.	4.66
224.	2.57
250.	1.13

Ref. 31

E/M	$\sigma(10^{-16}cm^2)$
347.	1.74
588.	0.176
974.	0.022
1390.	0.004

Ref. 20

He–O^{3+}

E/M	$\sigma(10^{-16}cm^2)$
6.55	2.26
20.6	1.80
51.2	0.991
117.	0.408
273.	0.094
523.	0.018
1010.	0.002

Ref. 40

He–O^{6+}

E/M	$\sigma(10^{-16}cm^2)$
18.6	7.81
46.4	4.25
117.	1.52
284.	0.360
529.	0.081
912.	0.013
1740.	0.001

Ref. 40

He–O^{8+}

E/M	$\sigma_{tot}(10^{-16}cm^2)$
1.53	38.7

Ref. 37

E/M	$\sigma(10^{-16}cm^2)$
100.0	20.1
125.	16.1
150.	13.0
173.	8.45
200.	7.14
224.	3.43
249.	1.78
275.	1.93
300.	0.94

Ref. 31

Table 5. Theoretical charge transfer cross sections for nonhydrogenic atoms and ions (q > 2), (continued)

He-O^{8+}

E/M	$\sigma(10^{-16}cm^2)$
6.64	23.4
27.5	16.4
72.9	7.32
169.	2.46
337.	0.697
569.	0.228
1300.	0.018
2475.	0.001

Ref. 40

E/M	$\sigma(10^{-16}cm^2)$
554.	0.336
980.	0.030
1400.	0.004
2000.	0.001

Ref. 20

He-F^{9+}

E/M	$\sigma_{tot}(10^{-16}cm^2)$
1.53	42.9

Ref. 37

E/M	$\sigma(10^{-16}cm^2)$
346.	4.25
469.	0.923
711.	0.165

Ref. 20

He-Si^{14+}

E/M	$\sigma_{tot}(10^{-16}cm^2)$
1.53	63.8

Ref. 37

E/M	$\sigma(10^{-16}cm^2)$
301.	18.7
380.	8.09
509.	2.57
662.	0.858
824.	0.336
1015.	0.114

Ref. 32

He-Ar^{5+}

E/M	$\sigma_{tot}(10^{-16}cm^2)$
0.750	28.0

Ref. 42

He-Ar^{6+}

E/M	$\sigma(10^{-16}cm^2)$
0.050	29.1
0.222	29.0
0.877	28.9
1.82	28.8
2.50	29.0

Ref. 3

He-Ar^{6+}

E/M	$\sigma(10^{-16}cm^2)$
0.061	28.3
0.081	27.2
0.112	26.3
0.203	24.8
0.434	23.1
0.886	21.5
1.32	20.5
1.97	19.5

Ref. 4

He-Xe^{3+}

E/M	$\sigma(10^{-16}cm^2)$
4.75	3.87
13.2	3.87
33.5	2.68
68.0	1.21
147.	0.405
337.	0.076
752.	0.0077
1650.	0.0003

Ref. 40

He-Xe^{4+}

E/M	$\sigma(10^{-16}cm^2)$
3.27	7.07
11.9	7.00
33.5	4.76
80.0	2.11
200.	0.585
480.	0.090
900.	0.012

Ref. 40

He-Xe^{6+}

E/M	$\sigma(10^{-16}cm^2)$
1.94	18.3
7.44	17.6
23.6	11.9
73.5	4.67
176.	1.43
427.	0.302
858.	0.045
1750.	0.003

Ref. 40

He-Xe^{8+}

E/M	$\sigma(10^{-16}cm^2)$
1.30	30.4
9.17	26.7
28.1	18.2
75.0	8.50
190.	2.62
393.	0.726
803.	0.150
1600.	0.0128

Ref. 40

He-Xe^{10+}

E/M	$\sigma(10^{-16}cm^2)$
0.94	47.6
5.85	46.4
22.8	35.1
60.5	20.2
144.	9.13
300.	2.86
600.	0.710
1050	0.188
2030	0.017
3440	0.001

Ref. 40

Table 5. Theoretical charge transfer cross sections for nonhydrogenic atoms and ions ($q > 2$), (continued)

Li-He^{2+}

E/M	$\sigma(10^{-16}\,cm^2)$
0.101	31.6
0.158	48.8
0.248	73.5
0.304	85.9
0.400	96.9
0.639	111.
0.960	119.
1.36	118.
2.00	110.
2.83	111.
3.96	112.
5.10	108.
6.28	101.
7.77	88.0
9.26	73.7
11.6	53.3
15.1	34.2
16.0	30.6

Ref. 18

E/M	$\sigma(10^{-16}\,cm^2)$
2.00	131.
2.75	122.
5.50	111.
10.0	76.0
25.0	15.0

Ref. 43

Li-He^{2+}

E/M	$\sigma(10^{-16}\,cm^2)$
9.73	62.7
12.7	54.6
14.8	46.8
17.1	37.1
19.3	31.7

Ref. 8, (CTMC)

E/M	$\sigma(10^{-16}\,cm^2)$
50.9	2.58
75.2	1.31

Ref. 44

C-He^{2+}

E/M	$\sigma(10^{-16}\,cm^2)$
774.	0.0279
1315.	0.0078
2070.	0.0020
3100.	0.0004

Ref. 34

C-Li^{3+}

E/M	$\sigma(10^{-16}\,cm^2)$
777.	0.167
1340.	0.046
2230.	0.009
3114.	0.003

Ref. 34

N-O^{3+}

E/M	$\sigma_{sum}(10^{-16}\,cm^2)$
6.87	8.30
22.6	5.18
50.9	2.73
135.	0.665
275.	0.169
515.	0.036
1260.	0.003

Ref. 40

N-O^{6+}

E/M	$\sigma_{sum}(10^{-16}\,cm^2)$
6.88	29.3
23.0	18.3
64.9	7.23
182.	1.50
421.	0.305
1100.	0.027
2870.	0.002

Ref. 40

N-O^{8+}

E/M	$\sigma_{sum}(10^{-16}\,cm^2)$
6.81	46.7
20.9	34.8
69.5	15.5
188.	4.40
373.	1.47
990.	0.221
2584.	0.018

Ref. 40

Ne-He^{2+}

E/M	$\sigma_K(10^{-20}\,cm^2)$
400.	2.32
700.	4.57
1000.	5.29
1500.	4.55
2500.	2.26
4000.	0.694

Ref. 15, (SPM)

E/M	$\sigma_K(10^{-20}\,cm^2)$
400	3.32
700	5.25
100	5.89
1500	4.87
2500	2.35
4000	0.711

Ref. 15, (IPM)

Ne-Li^{3+}

E/M	$\sigma_{tot}(10^{-16}\,cm^2)$
397.	0.225
527.	0.308
630.	0.356
740.	0.386
873.	0.406
957.	0.409
1097.	0.393
1325.	0.354
1600.	0.292
1940.	0.218
2440.	0.144
3000.	0.094
3625.	0.059
4140.	0.041

Ref. 15, (IPM)

Table 5. Theoretical charge transfer cross sections for nonhydrogenic atoms and ions (q ≥ 2), (continued)

Ne-Li^{3+}

E/M	$\sigma_K(10^{-16}cm^2)$
396.	0.127
504.	0.192
645.	0.259
779.	0.296
879.	0.313
989.	0.319
1070.	0.320
1193.	0.309
1430.	0.276
1715.	0.229
2320.	0.140
3090.	0.080
3970.	0.042

Ref. 15, (SPM)

E/M	$\sigma(10^{-16}cm^2)$
1340.	0.261
2240.	0.095

Ref. 34

Ne-N^{7+}

E/M	$\sigma_{K-K}(10^{-20}cm^2)$
1000.	368.
1360.	343.

Ref. 45

Ne-O^{8+}

E/M	$\sigma_{K-K}(10^{-20}cm^2)$
1500.	368.
1880.	269.
2190.	195.

Ref. 45

Ne-F^{9+}

E/M	$\sigma_{K-K}(10^{-20}cm^2)$
1050.	516.
1320.	440.
1580.	360.

Ref. 45

Ne-Kr^{3+}

E/M	$\sigma(10^{-16}cm^2)$
0.001	2.82
0.020	3.94
0.033	4.37
0.050	4.48
0.0623	4.36
0.117	3.77
0.144	3.69
0.182	3.88
0.244	4.78
0.350	6.34
0.775	8.35
1.36	9.27

Ref. 46

Ne-Xe^{2+}

E/M	$\sigma_{sum}(10^{-16}cm^2)$
2.82	1.67
12.8	1.35
47.4	0.793
124.	0.367
221.	0.176
442.	0.050
948.	0.001

Ref. 40

Ne-Xe^{4+}

E/M	$\sigma_{sum}(10^{-16}cm^2)$
2.26	7.15
14.5	4.16
69.5	1.65
231.	0.562
474.	0.190
909.	0.050
2070.	0.007

Ref. 40

Ne-Xe^{8+}

E/M	$\sigma_{sum}(10^{-16}cm^2)$
1.13	30.9
5.09	25.1
19.0	14.5
97.1	5.49
450.	1.35
1030.	0.411
2000.	0.095

Ref. 40

Ne-Xe^{10+}

E/M	$\sigma_{sum}(10^{-16}cm^2)$
0.822	53.5
6.72	42.4
56.5	23.1
194.	11.0
500.	4.30
1170.	1.30
2170.	0.373
3900.	0.067
8930.	0.005

Ref. 40

Si-F^{9+}

E/M	$\sigma_{K-K}(10^{-16}cm^2)$
370.	0.0062
580.	0.0117
785.	0.0173
1030.	0.0238
1340.	0.0299
1620.	0.0336
1950.	0.0329
2300.	0.0307
2600.	0.0278

Ref. 49

Si-Si^{14+}

E/M	$\sigma(10^{-16}cm^2)$
168.	0.0004
360.	0.0047
791.	0.0177
1190.	0.0255
1530.	0.0283
1860.	0.0279
2580.	0.0235
4570.	0.0114
7670.	0.0033

Ref. 21

Ar-He^{2+}

E/M	$\sigma_K(10^{-16}cm^2)$
1000.	0.0466
2500.	0.0724
5000.	0.0670
9000.	0.0308

Ref. 16

Table 5. Theoretical charge transfer cross sections for nonhydrogenic atoms and ions (q > 2), (continued)

Ar-C^{6+}

E/M	$\sigma_K(10^{-20}cm^2)$
1000.	5.43
2500.	18.6
5000.	12.1
9000.	4.81

Ref. 16

E/M	$\sigma_{K-K}(10^{-20}cm^2)$
1050.	1.30
1580.	2.52
1880.	5.40

Ref. 45

Ar-N^{7+}

E/M	$\sigma_{K-K}(10^{-20}cm^2)$
1050.	5.10
1880.	12.6

Ref. 45

Ar-F^{7+}

E/M	$\sigma_{sum}(10^{-16}cm^2)$
6.16	40.2
32.6	24.3
146.	8.45
530.	1.79
1100.	0.434
2395.	0.038

Ref. 40

Ar-F^{9+}

E/M	$\sigma_{K-K}(10^{-20}cm^2)$
1050.	5.6
1600.	10.0
1900.	16.0
2400.	22.0
3000.	26.0
3500.	27.0
4200.	27.0
6000.	21.0

Ref. 49

Ar-Ar^{6+}

E/M	$\sigma_{tot}(10^{-16}cm^2)$
0.055	115.
0.147	107.
0.362	100.
0.894	92.8
1.90	87.3
3.35	83.3

Ref. 42

Ar-Ar^{7+}

E/M	$\sigma_{tot}(10^{-16}cm^2)$
0.059	130.
0.235	117.
0.675	107.
1.49	100.
3.31	93.8

Ref. 42

Sc-Si^{14+}

E/M	$\sigma_{K-K}(10^{-20}cm^2)$
1930.	78.0

Ref. 19

Ti-He^{2+}

E/M	$\sigma_K(10^{-20}cm^2)$
2000.	0.0095
4000.	0.0099
6000.	0.0099
8000.	0.0093

Ref. 17

Ti-He^{2+}

E/M	$\sigma_L(10^{-20}cm^2)$
2000.	19.3
4000.	3.66
6000.	0.912
8000.	0.290

Ref. 17

Cu-He^{2+}

E/M	$\sigma_K(10^{-20}cm^2)$
6070.	0.00129

Ref. 17

Cu-He^{2+}

E/M	$\sigma_L(10^{-20}cm^2)$
6070.	0.833

Ref. 17

Cu-C^{6+}

E/M	$\sigma_K(10^{-20}cm^2)$
6070.	0.279

Ref. 17

Cu-C^{6+}

E/M	$\sigma_L(10^{-20}cm^2)$
6070.	89.7

Ref. 17

Cu-O^{8+}

E/M	$\sigma_K(10^{-20}cm^2)$
6070.	1.21

Ref. 17

Table 5. Theoretical charge transfer cross sections for nonhydrogenic atoms and ions ($q > 2$), (continued)

Cu-O^{8+}

E/M	$\sigma_L(10^{-20}cm^2)$
6070.	214.

Ref. 17

Cu-S^{16+}

E/M	$\sigma_{K-K}(10^{-20}cm^2)$
1710.	3.20

Ref. 19

Cu-Cl^{17+}

E/M	$\sigma_{K-K}(10^{-20}cm^2)$
1710.	4.20

Ref. 19

Kr-F^{9+}

E/M	$\sigma_{K-K}(10^{-20}cm^2)$
2420.	0.074
2950.	0.079
3470.	0.075
4000.	0.068

Ref. 45

Kr-Cl^{17+}

E/M	$\sigma_{tot}(10^{-20}cm^2)$
2820.	1.55
3390.	1.40
3950.	1.62
4510.	2.50

Ref. 45

Table 5. Theoretical cross sections for nonhydrogenic atoms and ions ($q \geq 2$), (continued)

$A + B^{Z+} \rightarrow A^{+} + B^{(Z-1)+}$

σ_{tot} (10^{-14} cm^2) at E = 1.53 keV/u. Ref. 37

A / B	He	Ne	Ar	Kr	Xe
B	0.262	0.394	0.75	1.13	1.31
C	0.304	0.500	0.87	1.28	1.51
N	0.346	0.505	0.99	1.43	1.72
O	0.387	0.561	1.11	1.58	1.93
F	0.429	0.616	1.23	1.73	2.13
Ne	0.471	0.672	1.35	1.88	2.34
Na	0.513	0.728	1.47	2.03	2.55
Mg	0.555	0.783	1.59	2.18	2.75
Al	0.596	0.839	1.71	2.33	2.96
Si	0.638	0.894	1.83	2.48	3.17
P	0.680	0.950	1.95	2.63	3.37
S	0.722	1.006	2.07	2.78	3.58
Cl	0.764	1.06	2.19	2.93	3.78
Ar	0.805	1.12	2.31	3.08	4.00
K	0.847	1.17	2.43	3.23	
Ca	0.889	1.23	2.55	3.38	
Sc	0.931	1.28	2.67	3.53	
Ti	0.973	1.34	2.79	3.68	
V	1.014	1.39	2.91	3.83	
Cr	1.056	1.45	3.03	3.98	
Mn	1.10	1.51	3.15	4.13	

$B + Ar^{q+} \rightarrow B^{+} + Ar^{(q-1)+}$

σ_{tot} (10^{-14} cm^2) at E = 0.76 keV/u. Ref. 42

q / B	3	4	5	6	7	8	9
He	19.2	23.3	28.0	32.6	37.5	42.0	45.8
Ne	25.1	31.6	38.4	44.9	51.2	57.2	63.5
Xe	91.8	114.	137.	159.	182.	203.	226.

$Kr + Xe^{+q} \rightarrow Kr^{+} + Xe^{(q-1)+}$

σ_{tot} (10^{-16} cm^2) at E = 0.23 keV/u. Ref. 42

q	3	4	5	6	7	8	9
	78.0	95.3	112	129	147	163	179

Table 5. Theoretical cross sections for nonhydrogenic atoms and ions ($q \geq 2$), (continued)

$A + B^{Z+} \rightarrow A^{+} + B^{(Z-1)+}$ σ_{tot} (10^{-14} cm^2) at E = 1.32 keV/u.				Ref. 37	
A / B	Li	Na	K	Rb	Cs
B	4.58	4.80	7.98	7.97	9.28
C	5.38	5.58	9.09	9.19	10.5
N	6.18	6.35	10.2	10.4	12.2
O	6.98	7.13	11.3	11.6	13.6
F	7.78	7.90	12.4	12.9	15.0
Ne	8.58	8.61	13.5	14.1	16.4
Na	9.38	9.44	14.6	15.3	17.8
Mg	10.2	10.2	15.7	16.5	19.2
Al	11.0	11.0	16.8	17.6	20.6
Si	11.8	11.8	17.9	19.0	22.0
P	12.6	12.6	19.1	20.2	23.4
S	13.4	13.4	20.2	21.4	24.8
Cl	14.2	14.3	21.3	22.6	26.2
Ar	15.0	15.1	22.4	23.9	27.6
K	15.8	15.9	23.5	25.1	29.1
Ca	16.6	16.7	24.6	26.3	30.5
Sc	17.4	17.5	25.7	27.5	31.9
Ti	18.2	18.3	26.8	28.8	33.3
V	19.0	19.1	27.9	30.0	34.7
Cr	19.8	20.0	29.0	31.2	36.1
Mn	20.6	20.8	30.1	32.4	37.5
Fe	21.4	21.6	31.2	33.6	38.9
Co	22.2	22.4	32.3	34.9	40.3
Ni	23.0	23.2	33.4	36.1	41.7
Cu	23.8	24.0	34.5	37.3	43.1
Zn	24.6	24.8	35.7	38.5	44.5
Ga	25.4	25.6	36.8	39.8	45.9
Ge	26.2	26.4	37.9	41.0	47.3
As	27.0	27.2	39.0	42.2	48.7
Se	27.8	28.0	40.1	43.4	50.1
Br	28.6	28.8	41.2	44.7	51.5
Kr	29.4	29.6	42.3	45.9	
Rb	30.2	30.4	43.4	47.1	
Sr	31.0	31.2	44.5	48.3	
Y	31.8	32.0	45.6	49.6	
Zr	32.6	32.9	46.7	50.8	

Table 6.a. Theoretical cross sections for one-electron charge transfer in ion-ion collisions

$He^{2+}-He^{+}$

E/M (keV/u)	σ (10^{-16} cm^2)
0.0042	0.943
0.0051	0.185
0.0061	0.514
0.0077	1.94
0.0090	4.43
0.0114	6.13
0.0129	7.06
0.0177	7.82
0.0248	8.44
0.0270	8.96
0.0357	9.09
0.0409	9.19
0.0485	9.28
0.0609	9.16
0.0715	9.19
0.0856	9.27
0.106	9.04
0.164	8.53
0.565	7.41
1.90	6.26
5.74	5.04
22.4	3.32

Ref. 25

$Li^{3+}-Li^{2+}$

E/M (keV/u)	σ (10^{-16} cm^2)
0.0135	0.790
0.0162	0.210
0.0177	0.358
0.0195	1.24
0.0267	2.34
0.0342	2.91
0.0454	3.30
0.0766	3.67
0.116	3.79
0.219	3.70
0.983	3.14
4.41	2.51
22.1	1.92

Ref. 25

$Be^{4+}-Be^{3+}$

E/M (keV/u)	σ (10^{-16} cm^2)
0.0237	0.152
0.0434	0.928
0.0549	1.45
0.0601	1.56
0.0833	1.59
0.120	1.88
0.173	2.00
0.368	1.82
1.88	1.53
8.88	1.26
35.2	0.997

Ref. 25

$B^{5+}-B^{4+}$

E/M (keV/u)	σ (10^{-16} cm^2)
0.0475	0.0167
0.0498	0.0243
0.0514	0.114
0.0624	0.470
0.0776	0.687
0.107	0.925
0.155	1.09
0.212	1.16
0.290	1.20
0.348	1.22
0.505	1.21
0.985	1.16
2.33	1.06
5.01	0.903
9.55	0.793
16.5	0.708

Ref. 25

$C^{6+}-C^{5+}$

E/M (keV/u)	σ (10^{-16} cm^2)
0.0889	0.0205
0.0938	0.0561
0.115	0.253
0.149	0.510
0.219	0.664
0.331	0.759
0.481	0.800
0.802	0.796
1.90	0.727
5.73	0.636
13.7	0.544
25.3	0.472

Ref. 25

$N^{7+}-N^{6+}$

E/M (keV/u)	σ (10^{-16} cm^2)
0.114	0.0166
0.125	0.0542
0.139	0.0158
0.196	0.0294
0.326	0.485
0.487	0.550
0.628	0.578
0.843	0.582
1.46	0.569
5.63	0.481
14.4	0.392
30.6	0.314

Ref. 25

$O^{8+}-O^{7+}$

E/M (keV/u)	σ (10^{-16} cm^2)
0.152	0.152
0.201	0.620
0.205	0.135
0.225	0.213
0.355	0.334
0.634	0.412
0.867	0.430
1.95	0.413
4.39	0.387
8.65	0.347
16.2	0.288
23.0	0.245

Ref. 25

Table 6.a. Theoretical cross sections for one-electron charge transfer in ion-ion collisions (continued)

$He^{2+}-O^{2+}$

E/M (keV/u)	σ (10^{-16} cm^2)
0.0213	1.13
0.0325	2.13
0.0519	3.59
0.0672	4.60
0.104	5.62
0.145	5.99
0.176	6.11
0.212	6.19
0.260	6.26
0.329	6.30
0.430	6.32
0.590	6.34
0.861	6.33
1.39	6.25
2.55	6.06
5.88	5.71
15.7	5.30

Ref. 27

$C^{2+}-B^{+}$

0.0400	2.70
0.0717	3.57
0.102	3.99
0.171	4.37
0.215	4.43
0.268	4.43
0.344	4.43
0.442	4.40
0.620	4.36
0.954	4.25
1.62	4.13
2.67	4.01
5.16	3.85
12.0	3.60
27.4	3.34

Ref. 27

$N^{3+}-C^{2+}$

0.0155	2.01
0.0273	3.36
0.0527	4.48
0.0977	5.10
0.172	5.37
0.203	5.38
0.239	5.38
0.272	5.39
0.318	5.38
0.382	5.37
0.466	5.34
0.587	5.29
0.770	5.23
1.01	5.14
1.41	5.02
2.21	4.88
3.62	4.71
7.28	4.53
21.1	4.20

Ref. 27

$O^{4+}-N^{3+}$

0.0201	1.20
0.0285	2.17
0.0390	2.80
0.0666	3.41
0.155	3.83
0.584	3.80
1.06	3.68
1.36	3.62
1.71	3.56
2.20	3.49
3.04	3.40
4.31	3.30
6.81	3.17
12.7	3.04
22.1	2.92

Ref. 27

$F^{5+}-O^{4+}$

0.0134	2.85
0.0190	3.69
0.0285	4.22
0.0524	4.54
0.154	4.66
0.412	4.55
0.499	4.47
0.643	4.40
0.775	4.37
0.991	4.28
1.24	4.22
1.74	4.13
2.37	4.04
3.59	3.89
6.20	3.71
12.6	3.45
25.5	3.18

Ref. 27

$Ne^{6+}-F^{5+}$

0.0268	0.0172
0.0311	0.620
0.0394	1.32
0.0517	1.86
0.0688	2.24
0.0983	2.57
0.135	2.81
0.202	3.03
0.309	3.17
0.536	3.21
0.680	3.21
0.906	3.18
1.30	3.15
1.72	3.09
2.16	3.04
3.42	2.94
5.05	2.84
7.60	2.74
12.6	2.59
19.6	2.45

Ref. 27

$O^{+}-C^{6+}$

0.146	0.220
0.729	3.00

Ref. 51

$C-N^{7+}$

0.155	0.00120
0.774	0.530

Ref. 51

Table 6.a. Theoretical cross sections for one-electron charge transfer in ion-ion collisions (continued)

$C^{3+}-N^{7+}$

E/M (keV/u)	σ (10^{-16}cm^2)
0.155	0.0120
0.774	0.0056

Ref. 51

$N^{+}-N^{7+}$

0.143	1.50
0.714	0.650

Ref. 51

$O^{2+}-N^{7+}$

0.134	15.0
0.669	16.0

Ref. 51

$N^{3+}-O^{8+}$

0.134	14.0
0.669	9.00

Ref. 51

$O^{+}-O^{8+}$

0.125	29.0
0.625	18.0

Ref. 51

$O^{3+}-O^{8+}$

E/M (keV/u)	σ (10^{-16}cm^2)
0.125	8.00
0.625	4.60

Ref. 51

$He^{2+}-He^{+}$

100.	0.208
126.	0.187
151.	0.157
176.	0.892
225.	0.612
251.	0.252
275.	0.180
300.	0.147

Ref. 52

$He^{2+}-O^{3+}$

250.	0.280
300.	0.311
350.	0.157
400.	0.405
450.	0.031
500.	0.034

Ref. 53

$He^{2+}-O^{4+}$

E/M (keV/u)	σ (10^{-16}cm^2)
250.	0.205
300.	0.164
350.	0.164
400.	0.0427
450.	0.0430
500.	0.0278

Ref. 53

$He^{2+}-O^{5+}$

250.	0.134
300.	0.0659
350.	0.114
400.	0.0307
450.	0.0281
500.	0.0193

Ref. 53

$He^{2+}-He^{+}$

100.	1.27
150.	0.413
250.	0.0843
375.	0.0203
500.	0.0067

Ref. 29, ($\sigma_{1S,1S}$)

$He^{2+}-He^{+}$

E/M (keV/u)	σ (10^{-16}cm^2)
100.	0.235
150.	0.839
250.	0.174
375.	0.395
500.	0.127

Ref. 29, ($\sigma_{1s,2s}$)

$He^{2+}-Li^{2+}$

100.	0.829
150.	0.408
250.	0.126
375.	0.040
500.	0.016

Ref. 29, ($\sigma_{1S,1S}$)

$He^{2+}-Li^{2+}$

100.	0.0448
150.	0.0376
250.	0.0159
375.	0.0058
500.	0.0024

Ref. 29, ($\sigma_{1S,2S}$)

$He^{2+}-Be^{3+}$

100.	0.0768
150.	0.0943
250.	0.0645
375.	0.0316
500.	0.0161

Ref. 29, ($\sigma_{1S,1S}$)

Table 6.a. Theoretical cross sections for one-electron charge transfer in ion-ion collisions (continued)

He^{2+}–Be^{3+}

E/M (keV/u)	σ (10^{-16} cm^2)
150.	0.0047
250.	0.0059
375.	0.0037
500.	0.0020

Ref. 25, ($\sigma_{1S,2S}$)

He^{2+}–Li^{+}

25.	41.3
125.	1.83
250.	0.303
500.	0.0319
1000.	0.0021

Ref. 24

Ba^{+}–Ba^{+}

0.20	1.46
0.32	3.76
0.43	5.36
0.53	6.63
0.57	7.03
0.79	8.05
1.25	10.6
1.61	13.2
1.98	16.2
2.27	18.6
2.47	19.9
2.68	21.1
2.87	21.9
3.12	22.7
3.42	23.3
3.64	23.5

Ref. 28

Table 6.b. Theoretical cross sections for two-electron charge transfer in ion-ion collisions. All data were taken from Ref. 26

$Li^{3+}-Li^{+}$

E/M (keV/u)	σ (10^{-16} cm^2)
0.012	0.382
0.018	0.838
0.026	1.11
0.037	1.27
0.050	1.39
0.066	1.46
0.079	1.48
0.112	1.49
0.154	1.49
0.241	1.46
0.753	1.32
2.62	1.16
10.4	0.974
30.5	0.820

$Be^{4+}-Be^{2+}$

E/M (keV/u)	σ (10^{-16} cm^2)
0.024	0.017
0.037	0.295
0.064	0.614
0.087	0.760
0.127	0.843
0.200	0.891
0.292	0.904
0.562	0.890
1.90	0.820
6.57	0.722
14.4	0.661
22.8	0.617

$B^{5+}-B^{3+}$

E/M (keV/u)	σ (10^{-16} cm^2)
0.046	0.016
0.076	0.240
0.126	0.409
0.191	0.523
0.234	0.568
0.335	0.605
0.510	0.620
0.807	0.614
2.23	0.580
8.38	0.517
24.2	0.458

$C^{6+}-C^{4+}$

E/M (keV/u)	σ (10^{-16} cm^2)
0.073	0.031
0.131	0.210
0.214	0.326
0.340	0.406
0.500	0.430
0.747	0.443
1.17	0.446
2.85	0.429
9.84	0.395
24.0	0.365

$N^{7+}-N^{5+}$

E/M (keV/u)	σ (10^{-16} cm^2)
0.164	0.093
0.220	0.187
0.323	0.251
0.458	0.292
0.670	0.323
0.941	0.342
1.30	0.351
1.88	0.353
2.75	0.350
5.37	0.338
9.70	0.325
19.7	0.308
36.0	0.289
54.9	0.277

$O^{8+}-O^{6+}$

E/M (keV/u)	σ (10^{-16} cm^2)
0.236	0.094
0.326	0.157
0.466	0.205
0.662	0.240
0.941	0.263
1.34	0.275
2.00	0.281
2.76	0.283
4.35	0.280
8.67	0.271
16.1	0.261
31.9	0.247
51.7	0.237

$F^{9+}-F^{7+}$

E/M (keV/u)	σ (10^{-16} cm^2)
0.266	0.071
0.387	0.130
0.568	0.174
0.733	0.197
0.965	0.214
1.28	0.225
2.22	0.233
3.68	0.234
8.23	0.228
19.2	0.216
40.3	0.205

$Ne^{10+}-Ne^{8+}$

E/M (keV/u)	σ (10^{-16} cm^2)
0.366	0.063
0.610	0.117
0.867	0.147
1.18	0.163
1.66	0.176
2.25	0.183
3.79	0.185
6.42	0.183
12.7	0.178
24.2	0.172
38.5	0.167

Table 6.b. Theoretical cross sections for two-electron charge transfer in ion-ion collisions (continued)
All data were taken from Ref. 26.

$B^{3+}-B^{+}$

E/M (keV/u)	σ (10^{-16} cm^2)
0.003	2.20
0.004	4.04
0.005	6.29
0.007	7.69
0.010	8.57
0.017	9.28
0.025	9.52
0.038	9.57
0.068	9.33
0.153	8.84
0.424	7.96
1.22	7.11
1.76	6.75
2.24	6.65
2.81	6.44
3.65	6.23
4.88	5.96
6.41	5.65
9.58	5.35
15.5	4.96
29.4	4.40
46.2	4.05

$C^{4+}-C^{2+}$

E/M (keV/u)	σ (10^{-16} cm^2)
0.010	1.78
0.015	3.63
0.022	4.77
0.036	5.54
0.052	5.97
0.069	6.15
0.096	6.19
0.204	5.98
0.427	5.72
0.924	5.36
2.15	4.99
4.07	4.68
6.31	4.42
11.0	4.16
22.6	3.84
33.9	3.65

$N^{5+}-N^{3+}$

E/M (keV/u)	σ (10^{-16} cm^2)
0.027	2.17
0.043	3.14
0.073	3.89
0.109	4.18
0.168	4.30
0.407	4.24
0.956	4.00
1.88	3.83
3.93	3.53
7.74	3.31
16.5	3.08
36.2	2.85

$O^{6+}-O^{4+}$

E/M (keV/u)	σ (10^{-16} cm^2)
0.042	1.54
0.074	2.46
0.163	3.03
0.323	3.19
0.743	3.11
2.29	2.92
4.52	2.81
9.25	2.63
22.6	2.45
35.1	2.37

Table 7. Theoretical data for double charge transfer in ion-atom collisions

He–He^{2+}

E/M (keV/amu)	σ (10^{-16} cm^2)
0.049	4.88
0.108	4.28
0.167	3.93
0.220	3.75
0.250	3.71

Ref. 55

0.26	3.35
0.70	3.08
2.04	2.34
3.22	2.09
4.65	1.91
5.94	1.82
6.75	1.77

Ref. 56

0.373	2.29
0.947	2.03
1.69	1.87
2.58	1.73
3.50	1.63
4.74	1.53
6.27	1.45
7.47	1.40
9.07	1.34
11.1	1.30
11.7	1.29

Ref. 30

He–He^{2+}

E/M (keV/amu)	σ (10^{-16} cm^2)
2.30	2.11
3.02	1.96
4.62	1.84
7.25	1.64
8.54	1.54
10.6	1.39
13.5	1.16
16.3	1.01
21.2	0.861
26.7	0.801
31.4	0.750
34.5	0.720
36.0	0.708

Ref. 5

34.1	0.678
56.5	0.294
77.3	0.153
100.	0.0786
122.	0.0432
143.	0.0251
163.	0.0150
182.	0.0088
200.	0.0056
215.	0.0038
223.	0.0029

Ref. 57

15.9	0.917
19.6	0.938
30.9	0.879
50.3	0.632
87.3	0.220
126.	0.0708
194.	0.0136
252.	0.0042
314.	0.0016
344.	0.0011

Ref. 29

He–He^{2+}

E/M (keV/amu)	σ (10^{-16} cm^2)
125.	0.130
188.	0.011
250.	0.0017

Ref. 58

He–C^{4+}

0.006	1.33
0.009	1.92
0.017	2.59
0.032	3.50
0.065	4.19
0.102	4.45
0.139	4.31
0.260	4.09
0.658	3.32
1.45	2.66
2.75	2.16
4.34	1.81
5.88	1.61
7.33	1.50

Ref. 30

0.220	4.14
0.427	3.58
0.791	3.05
1.60	2.41
2.90	1.96
4.35	1.69
5.09	1.61
5.31	1.58

Ref. 6

He–Ar^{6+}

E/M (keV/amu)	σ (10^{-16} cm^2)
0.049	6.88
0.248	6.86
1.07	6.84
2.50	6.78

Ref. 3

Ne–N^{7+}

380.	0.0049
580.	0.0039
722.	0.0033
967.	0.0026
1220.	0.0019
1400.	0.0015
1620.	0.0012

Ref. 57

Ne–O^{8+}

346.	0.0085
507.	0.0071
746.	0.0056
1110.	0.0039
1470.	0.0026
1730.	0.0020
2000.	0.0016

Ref. 57

Table 7. Theoretical data for double charge transfer in ion-atom collisions (continued)

Ne–F^{9+}

E/M (keV/amu)	σ (10^{-16} cm^2)
221.	0.0109
723.	0.0070
1110.	0.0050
1430.	0.0038
1960.	0.0024
2510.	0.0014
3070.	0.0009
3450.	0.0007
3650.	0.0006
3840.	0.0005

Ref. 57

Ar–F^{9+}

1600.	0.200
1840.	0.110
2110.	0.059
2370.	0.034
2630.	0.021
2900.	0.013
3260.	0.007

Ref. 58

6. Acknowledgments

One of us (RKJ) would like to express his gratitude to the staff of the Joint Institute for Laboratory Astrophysics (JILA) for the hospitality extended to him while this work was performed. We are indebted to the personnel of the JILA Data Center for the highly professional assistance and to the personnel of the JILA Scientific Reports Office for their help in preparation of the manuscript. The partial support to this work by the National Bureau of Standards [Contracts No. NBS(G)-279-YU and NB82 RAC 20031] and the International Atomic Energy Agency, Vienna, Austria (Contract No. 2857/R2/RB with RKJ) is gratefully acknowledged.

7. References

[1]R. K. Janev, B. H. Bransden, and J. W. Gallagher, J. Phys. Chem. Ref. Data **12**, 829 (1983).
[2]J. W. Gallagher, B. H. Bransden, and R. K. Janev, J. Phys. Chem. Ref. Data **12**, 873 (1983).
[3]R. K. Janev and L. P. Presnyakov, Phys. Rep. **70**, 1 (1981).
[4]T. P. Grozdanov and R. K. Janev, J. Phys. (Paris) Colloq. C7 **40**, 71 (1979).
[5]C. Harel and A. Salin, J. Phys. B **13**, 785 (1980).
[6]E. J. Shipsey, J. C. Browne, and R. E. Olson, Phys. Rev. A **15**, 2166 (1977).
[7]R. E. Olson, E. J. Shipsey, and J. C. Browne, in *Abstracts of Papers of the IXth International Conference on the Physics of Electronic and Atomic Collisions*, Seattle, Washington, July 1975; edited by J. S. Risley and R. Geballe (University of Washington, Seattle, WA, 1975), p. 101.
[8]E. J. Shipsey, L. T. Redmond, J. C. Browne, and R. E. Olson, Phys. Rev. A **18**, 1961 (1978).
[9]L. Opradolce, P. Valiron, and R. McCarroll in *Abstracts of Contributed Papers of the XIth International Conference on the Physics of Electronic and Atomic Collisions*, Kyoto, Japan, August 1979; edited by K. Takayanagi and N. Oda (North–Holland, Amsterdam, 1979), p. 564.
[10]B. Hird and S. P. Ali, Can. J. Phys. **58**, 772 (1980).
[11]R. K. Janev, Phys. Rev. A **28**, 1810 (1983).
[12]R. K. Janev and P. Hvelplund, Comm. At. Mol. Phys. **11**, 75 (1981).
[13]F. Herman and S. Skillman, *Atomic Structure Calculations* (Prentice–Hall, Englewood Cliffs, NJ, 1963).
[14]J. Eichler, W.Fritsch, and U. Wille, Phys.Rev. A **20**, 1448 (1979).
[15]A. L. Ford, J .F. Reading, and R. L. Becker, Phys. Rev. A **23**, 510 (1981).
[16]R. L. Becker, A. L. Ford and J. F. Reading, J. Phys. B **13**, 4059 (1980).
[17]J. F. Reading, A. L. Ford, G. L. Swafford, and A. Fitchard, Phys. Rev. A **20**, 130 (1979).
[18]W. Fritsch and C. D. Lin, J. Phys. B **16**, 1595 (1983).
[19]C. D. Lin in *Abstracts on Contributed Papers of the XIth International Conference on the Physics of Electronic and Atomic Collisions*, Kyoto, Japan, August, 1979; edited by K. Takayanagi and N. Oda (North–Holland, Amsterdam, 1979), p. 568.
[20]J. A. Guffey, L. D. Ellsworth, and J. R. McDonald, Phys. Rev. A **15**, 1863 (1977).
[21]V. P. Shevelko, J. Phys. B **13**, L319 (1980).
[22]Dz. S. Belkić and R. K. Janev, J. Phys. B **6**, 1020 (1973).
[23]Dz. S. Belkić and R. Gayet, J. Phys. B **10**, 1923 (1977).
[24]G. W. Shirteliffe and K. E. Banyard, Phys. Rev. A **21**, 1197 (1980).
[25]V. P. Zhdanov, Sov. Phys. Tech. Phys. **21**, 117 (1976).
[26]R. K. Janev and D. S. Belic, Phys. Lett. A **89**, 190 (1982).
[27]R. K. Janev and D. S. Belic, J. Phys. B **15**, 3487 (1982).
[28]S. J. Sramek and J. H. Macek, Phys. Rev. A **22**, 1467 (1980).
[29]S. Muckerjee and N. C. Sil, J. Phys. B **13**, 3421 (1980).
[30]T. P. Grozdanov and R. K. Janev, J. Phys. B **13**, 3431 (1980).
[31]R. E. Olson, Phys. Rev. A **18**, 2464 (1978).
[32]H. Tawara, Phys. Lett. A **71**, 208 (1979).
[33]T. C. Theisen and J. H. McGuire, Phys. Rev. A **20**, 1406 (1979).
[34]T. S. Ho, M. Lieber, F. T. Chan, and K. Omidvar, Phys. Rev. A **24**, 2933 (1981).
[35]Y. Kajikawa, N. Toshima, T. Watanabe, and H. Ryufuku, in *ICPEAC XII: Abstracts of Contributed Papers of the XIIth International Conference on the Physics of Electronic and Atomic Collisions*, Gatlinburg, TN, 15–21 July 1982, edited by S. Datz (North–Holland, Amsterdam, 1981), Vol. 2, p. 682.
[36]V. Malaviya, Proc. Indian Natl. Sci. Acad. Part A **39**, 458 (1973).
[37]T. P. Grozdanov and R. K. Janev, Phys. Rev. A **17**, 880 (1978).
[38]G. Steigman, Astrophys. J. **199**, 336 (1975).
[39]B. Hird, H. C. Suk, and S. P. Ali, Can. J. Phys. **57**, 2078 (1979).
[40]V. P. Shevelko, Z. Phys. A **287**, 19 (1978).
[41]F. T. Chan and J. Eichler, Phys. Rev. A **20**, 1841 (1979).
[42]T. P. Grozdanov and R. K. Janev, Phys. Lett. A **66**, 191 (1978).
[43]B. H. Bransden and A. M. Ermolaev, Phys. Lett. A **84**, 316 (1981).
[44]R. E. Olson, J. Phys. B **15**, L163 (1982).
[45]C. D. Lin, J. Phys. B **11**, L185 (1978).
[46]L. P. Presnyakov and A. D. Ulantsev, Kvant. Elektron. **1**, 2377 (1974) [Sov. J. Quant. Electron. **4**, 1320 (1975)].
[47]C. D. Lin, J. Phys. B **11**, L595 (1978).
[48]W. Fritsch, C. D. Lin, and L. N. Tunnell, J. Phys. B **14**, 2861 (1981).
[49]C. D. Lin and L. N. Tunnell, Phys. Rev. A **22**, 76 (1980).
[50]M. I. Chibisov, Pisma Zh. Eksp. Teor. Fiz. **24**, 56 (1976) [JETP Lett. **24**, 46 (1976)].
[51]V. A. Bazylev and M. I. Chibisov, Fiz. Plazmy **5**, 584 (1979) [Sov. J. Plasma Phys. **5**, 327 (1979)].
[52]R. E. Olson, J. Phys. B **11**, L227 (1978).
[53]R. E. Olson, Phys. Lett. A **71**, 341 (1979).
[54]M. Lal, M. K. Srivastava, and A. N. Tripathi, Phys. Rev. A **26**, 305 (1982).
[55]R. D. Rivarola and R. D. Piacentini, Phys. Rev. A **20**, 1816 (1979).
[56]M. I. Chibisov, Zh. Eksp. Teor. Fiz. **70**, 1687 (1976) [Sov. Phys. JETP **43**, 879 (1976)].
[57]C. D. Lin, Phys. Rev. A **19**, 1510 (1979).
[58]R. Gayet, R. D. Rivarola, and A. Salin, J. Phys. B **14**, 2421 (1981).
[59]See Ref. 3.
[60]A. Itoh, M. Asari, and F. Fukuzawa, J. Phys. Soc. Japan **48**, 943 (1980).
[61]S. K. Allison, Phys. Rev. **109**, 76 (1958).
[62]K. H. Berkner, R. V. Pyle, J. W. Stearns, and J. C. Warren, Phys. Rev. **166**, 44 (1968).
[63]J. E. Bayfield and G. A. Khayrallah, Phys. Rev. A **11**, 920 (1975).
[64]G. R. Hertel and W. S. Koski, J. Chem. Phys. **40**, 3452 (1964).
[65]P. Hvelplund, J. Heinemeier, E. Horsdal Pedersen and F. R. Simpson, J. Phys. B **9**, 491 (1976).
[66]L. I. Pivovar, V. M. Tubaev, and M. T. Novikov, Zh. Eksp. Teor. Fiz. **41**, 26 (1961) [Sov. Phys. JETP **14**, 20 (1962)].
[67]M. B. Shah and H.B.Gilbody, J. Phys. B **9**, 1933 (1976).
[68]M. Matic, V. Sidis, B. Cobic, M. Vujovic in *ICPEAC XI: Abstracts of Contributed Papers of the XIth International Conference on the Physics of Electronic and Atomic Collisions*, Kyoto, Japan, 29 August–4 September 1979, edited by K. Takayanagi and N. Oda (North–Holland, Amsterdam, 1979), p. 546.
[69]V. S. Nikolaev, I. S. Dmitriev, L. N. Fateeva, and Ya. A. Teplova, Zh. Eksp. Teor. Fiz. **40**, 989 (1961) [Sov. Phys. JETP **13**, 695 (1961)].
[70]I. Wirkner-Bott, W. Seim, A. Müller, P. Kester, and E. Salzborn, J. Phys. B **14**, 3987 (1981).
[71]T. Iwai, Y. Kaneko, M. Kimura, N. Kobayashi, S. Ohtani, K. Okuno, S. Takagi, H. Tawara, and S. Tsurubuchi, Phys. Rev. A **26**, 105 (1982).
[72]D. H. Crandall, Phys. Rev. A **16**, 958 (1977).
[73]H. J. Zwally and P. G. Cable, Phys. Rev. A **4**, 2302 (1971).
[74]I. S. Dmitriev, V. S. Nikolaev, Yu. A. Tashaev, and Yu. A. Teplova, Zh. Eksp. Teor. Fiz. **67**, 2047 (1974) [Sov. Phys. JETP **40**, 1017 (1975)].
[75]V. V. Afrosimov, A. A. Basalaev, E. D. Donets, K. O. Lozhkin, and M. N. Panov, in *ICPEAC XII: Abstracts of Contributed Papers of the XIIth International Conference on the Physics of Electronic and Atomic Collisions*, Gatlinburg, TN, 15–21 July 1981, edited by S. Datz (North–Holland, Amsterdam, 1981), Vol. 2, p. 690.
[76]T. R. Dillingham, J. R. Macdonald, and P. Richard, Phys. Rev. A **24**, 1237 (1981)
[77]T. J. Gray, C. L. Cocke, and E. Justiniano, Phys. Rev. A **22**, 849 (1980).
[78]H. Knudsen, H. K. Haugen, and P. Hvelplund, Phys. Rev. A **23**, 597 (1981).
[79]H. Klinger, A. Muller, and E. Salzborn, J. Phys. B **8**, 230 (1975).
[80]G. A. Murray, J. Stone, M. Mayo, and T. J. Morgan, Phys. Rev. A **25**, 1805 (1982).
[81]R. W. McCullough, T. V. Goffe, M. B. Shah, M. Lennon, and H. B. Gilbody, J. Phys. B **15**, 111 (1982).
[82]K. Kadota, D. Dijkkamp, R. L. Van Der Woude, A. De Boer, P. G.Yan, and F. J. De Heer, J. Phys. B **15**, 3275 (1982).
[83]M. Rodbro, E. H. Pedersen, C. L. Cocke, and J. R. Macdonald, Phys. Rev. A **19**, 1936 (1979).

[84]C. L. Cocke, R. Du Bois, T. J. Gray, E. Justiniano, and C. Can, Phys. Rev. Lett. **46**, 1671 (1981).
[85]S. Bliman, S. Dousson, B. Jacquot, and D. Van Houtte, J. Phys. (Paris) **42**, 1387 (1981).
[86]H. Winter, T. M. El-Sherbini, E. Bloeman, F. J. De Heer, and A. Salop, Phys. Lett. A **68**, 211 (1978).
[87]A. Müller and E. Salzborn, Phys. Lett. A **59**, 19 (1976).
[88]V. V. Afrosimov, A. A. Basalaev, M. N. Panov, and G.A. Leiko, Pisma Zh. Eksp. Teor. Fiz. **26**, 699 (1977) [JETP Lett. **26**, 537 (1977)].
[89]M. B. Shah and H. B. Gilbody, J. Phys. B **7**, 256 (1974).
[90]S. L. Varghese, W.Waggoner, and C.L. Cocke, Phys. Rev. A **29**, 2453 (1984).
[91]V. V. Afrosimov, G. A. Leiko, Yu. A. Mamsev, and M. N. Panov, Sov. Phys. JETP **40**, 661 (1975).
[92]D. H. Crandall, R. E. Olson, E. J. Shipsey, and J. C. Browne, Phys. Rev. Lett. **36**, 858 (1976).